Journal of Medicinal Chemistry

Subscriber access provided by BALL STATE UNIV

Article

Discovery of Thieno[3,2-*d*]pyrimidine-6-carboxamides as potent inhibitors of SIRT1, SIRT2 and SIRT3.

Jeremy S. Disch, Ghotas Evindar, Cynthia H. Chui, Charles A. Blum, Han Dai, Lei Jin, Eli Schuman, Kenneth E. Lind, Svetlana L. Belyanskaya, Jianghe Deng, Frank T. Coppo, Leah Aquilani, Todd L. Graybill, John W. Cuozzo, Siva Lavu, Cheney Mao, George P. Vlasuk, and Robert Bruno Perni

J. Med. Chem., **Just Accepted Manuscript** • DOI: 10.1021/jm400204k • Publication Date (Web): 09 Apr 2013

Downloaded from http://pubs.acs.org on April 15, 2013

Just Accepted

"Just Accepted" manuscripts have been peer-reviewed and accepted for publication. They are posted online prior to technical editing, formatting for publication and author proofing. The American Chemical Society provides "Just Accepted" as a free service to the research community to expedite the dissemination of scientific material as soon as possible after acceptance. "Just Accepted" manuscripts appear in full in PDF format accompanied by an HTML abstract. "Just Accepted" manuscripts have been fully peer reviewed, but should not be considered the official version of record. They are accessible to all readers and citable by the Digital Object Identifier (DOI®). "Just Accepted" is an optional service offered to authors. Therefore, the "Just Accepted" Web site may not include all articles that will be published in the journal. After a manuscript is technically edited and formatted, it will be removed from the "Just Accepted" Web site and published as an ASAP article. Note that technical editing may introduce minor changes to the manuscript text and/or graphics which could affect content, and all legal disclaimers and ethical guidelines that apply to the journal pertain. ACS cannot be held responsible for errors or consequences arising from the use of information contained in these "Just Accepted" manuscripts.

ACS Publications
High quality. High impact.

Journal of Medicinal Chemistry is published by the American Chemical Society. 1155 Sixteenth Street N.W., Washington, DC 20036

Published by American Chemical Society. Copyright © American Chemical Society. However, no copyright claim is made to original U.S. Government works, or works produced by employees of any Commonwealth realm Crown government in the course of their duties.

Discovery of Thieno[3,2-*d*]pyrimidine-6-carboxamides as potent inhibitors of SIRT1, SIRT2 and SIRT3.

Jeremy S. Disch[*], *Ghotas Evindar*[†*], *Cynthia H. Chiu*[†], *Charles A. Blum, Han Dai, Lei Jin, Eli Schuman, Kenneth E. Lind*[†], *Svetlana L. Belyanskaya*[†], *Jianghe Deng*[‡], *Frank Coppo*[‡], *Leah Aquilani*[‡], *Todd L. Graybill*[‡], *John W. Cuozzo*[†], *Siva Lavu, Cheney Mao*[⊥], *George P. Vlasuk, and Robert B. Perni*

Sirtris a GSK Company, Cambridge, Massachusetts, United States

[†] ELT Boston, Platform Technology and Science, GlaxoSmithKline, Waltham, Massachusetts, United States

[‡] ELT UP, Platform Technology and Science, GlaxoSmithKline, Upper Providence, Pennsylvania, United States

[⊥] Viva Biotech Ltd., 334 Aidisheng Road, Zhangjiang High-tech Park, Shanghai, China

ABSTRACT

The sirtuins SIRT1, SIRT2 and SIRT3 are NAD^+ dependent deacetylases that are considered potential targets for metabolic, inflammatory, oncologic and neurodegenerative disorders. Encoded Library Technology (ELT) was used to affinity screen a 1.2 million heterocycle enriched library of DNA encoded small molecules, which identified pan-inhibitors of SIRT1/2/3 with nanomolar potency (e.g. **11c**: IC_{50} = 3.6, 2.7 and 4.0 nM for SIRT1, SIRT2 and SIRT3 respectively). Subsequent SAR studies to improve physiochemical properties identified the potent drug like analogs **28** and **31**. Crystallographic studies of **11c**, **28** and **31** bound in the SIRT3 active site revealed that the common carboxamide binds in the nicotinamide C-pocket and the aliphatic portions of the inhibitors extend through the substrate channel, explaining the observable SAR. These pan SIRT1/2/3 inhibitors, representing a novel chemotype, are significantly more potent than currently available inhibitors which makes them valuable tools for sirtuin research.

KEYWORDS

SIRT1, SIRT2, SIRT3, sirtuin inhibitor, pan SIRT1/2/3 inhibitor, thieno[3,2-*d*]pyrimidine-6-carboxamides, X-ray structure, Encoded Library Technology, ELT.

INTRODUCTION

In recent years, the sirtuins, a series of seven Class III NAD^+ dependent histone deacetylases, have been implicated as important regulators of numerous cellular processes and play physiological roles related to lifespan and aging.[1-2] Modulating sirtuin activity[3], either through overexpression (activation) or knockdown (inhibition), has been proposed to be beneficial in numerous disease states including those related to metabolism,[4] cancer,[5-6] neurodegeneration,[7-9] inflammation,[10-11] and ischaemic injury.[12] Currently our understanding of sirtuin function is far from complete. Conflicting reports abound even for SIRT1, which is by far the most studied of the seven sirtuins. For example, in one study SIRT1 knock-out mice displayed increased weight gain and decreased glucose tolerance.[13] While in another study, SIRT1 deficient mice showed increased glucose tolerance, decreased weight gain and lower fat accumulation in some tissues.[14] What is clear is that the function of these enzymes is dependent on their cellular localization and the type of tissue where the cells reside.[1]

Nevertheless, there is compelling evidence that sirtuin modulation could find significant clinical use. SIRT1 and SIRT2 both fulfill the same function of deacetylating p53, which is a tumor suppressor protein involved in regulating a pathway leading toward apoptosis. Though inactivating SIRT1 or SIRT2 individually was insufficient for inhibiting the deacetylation of p53 *in vivo*, the simultaneous inhibition of SIRT1 and SIRT2 was beneficial against cancer by completely blocking p53 deacetylation, which lead to cell death.[5] In a neurodegenerative setting, evidence suggests that the SIRT2 mediated deacetylation of FOXO3a promotes neuronal damage leading to apoptotic pathways, and that SIRT2 knockout prevents neuronal death in a Parkinson disease mouse model.[7]

One of the common structural features of all seven sirtuins is a largely conserved catalytic core while otherwise incorporating significantly variable C- and N-terminal regions. This conserved core leads to the assumption that it may be possible to identify pan inhibitors of these enzymes as a means of therapeutic intervention. Alternatively, it also suggests that it may be difficult to design selective active site inhibitors.

To date, there have been several reports identifying sirtuin inhibitors, largely focused on SIRT1 and SIRT2. Among the earliest SIRT1/2 inhibitors identified were sirtinol (**1**, Figure 1) and the closely related salermide (**2**), both which display marginal selectivity for SIRT2.[15-16] Suramin (**3**), a high molecular weight urea derivative, also inhibited SIRT1 and SIRT2 with little selectivity (IC_{50} = 0.3 μM and 1.2 μM respectively).[16] The tetrahydrocarbazole inhibitor, EX527 (**4**) on the other hand**,** is more selective for SIRT1 over SIRT2 and SIRT3.[17] This compound is among the most studied of the published inhibitors and has been used as a standard inhibitor in biological studies. Overall, a broad spectrum of compound classes have demonstrated sirtuin inhibition[18] ranging from peptide substrate mimetics (**5**)[19-21] to heterocyclic small molecules such as cambinol (**6**).[22] In general, these inhibitors exhibit micromolar or high nanomolar potencies and tend to have moderate selectivity for SIRT1.

More recently, selective SIRT2 inhibitors have been reported including 2-anilinobenzamide analogues (**7**) [23] and the chromanone derivative **8**.[24] Benzamide **7** exhibits >500:1 preference for SIRT2 over SIRT1 and SIRT3. Similarly, chromanone **8** shows selectivity over both SIRT1 and SIRT3, showing less than 10% inhibition at 200 μM against SIRT1/3. There is also a recent report[25] showing that 3-(1*H*-1,2,3-triazol-4-yl)pyridine, a nicotinamide analogue, was modestly selective for SIRT3 (IC_{50} = 38 μM) over SIRT1 and SIRT2 (88% and 92% activity remaining at 1 mM for SIRT1 and SIRT2 respectively), and it demonstrated modest antiproliferative effects against several cancer cell lines. Ultimately, the known classes of inhibitors all possess significant liabilities even as tool compounds. With the possible exception of **4**, they are generally poorly potent or suffer from poor physicochemical properties. In order to develop a complete understanding of sirtuin function, there is a need for better tool compounds composed of both sirtuin activators and inhibitors.

Herein, we report a new class of potent sirtuin inhibitors based on a thieno[3,2-*d*]pyrimidine-6-carboxamide scaffold, (**9**, Figure 2). These inhibitors were initially discovered through an *in vitro* SIRT3 affinity selection using Encoded Library Technology (ELT).[26] These compounds represent a

novel class of very potent, low nanomolar, pan SIRT1/2/3 inhibitors, which could serve as aids in elucidating the diverse biology of sirtuins.

RESULTS AND DISCUSSION

ELT Screening

In our efforts to discover novel small molecules that modulate sirtuin activity, we utilized Encoded Library Technology (ELT)[26-27], a novel and robust hit identification platform that employs large collections of chemotypically diverse DNA-encoded small molecule libraries which are screened for their affinity towards a desired protein target. The technology provides access to a broad set of chemotypes with vast structural diversity in an evolving library collection. It is also an attractive platform because it uses negligible amounts of target protein to carry out selection experiments, and it identifies ligands regardless of their functional activity. In the past few years, ELT has been successfully used to identify hits against a number of soluble targets.[28-32]

In pursuit of novel small molecule modulators of SIRT3, we carried out an ELT selection campaign against a Flag-SBP-tagged SIRT3 construct. Flag-SIRT3-SBP was immobilized on streptavidin matrix tips, and selections were performed under three conditions: SIRT3 alone; SIRT3 plus β-Nicotinamide Adenine Dinucleotide (NAD^+); and SIRT3 plus thioacetyl-peptide ACS2 substrate ($TRSGK_{s\text{-}Ac}VMRRLLR$).[33] These SIRT3 selection conditions were used to screen a 3-cycle linear library capped with heteroaryl moieties (**10**, Figure 3a). The library was established by coupling 16 bis-acid building blocks (cycle 1) to the ELT headpiece (HP) which allowed for further elaboration of the second carboxylate with 134 diamines (cycle 2). The second amine from cycle 2 was then functionalized with 570 heteroaryl building blocks (cycle 3) to afford an ELT library with 1.2 million enumerated compounds. The details of the synthesis of this novel encoded library will be the subject of a separate publication.

The library was screened against SIRT3 (see Experimental Methods) and the sequencing data was transferred into a cubic scatter plot for visualization and analysis within Spotfire™, where each axis

represents a cycle of diversity in the library (Figure 3b). The background noise, single hits, and low copy number molecules were removed to simplify the data analysis. This allowed for closer observation of the more highly enriched families and features within the cube.

The main selected chemotype was represented by a horizontal and a vertical line intersecting at a single point in the cube. These lines defined a plane in cycle 3 originating from the 4-chlorothieno[3,2-*d*]pyrimidine-6-carboxamide building block connected to cycle 2 through an amine displacement of the chloride. The horizontal and vertical lines, themselves, originated from a combination of the selected cycle 3 building block (4-chlorothieno[3,2-*d*]pyrimidine-6-carboxamide) and a specific cycle 1 (thiophene-2,5-dicarboxylic acid) or cycle 2 building block (2-(piperidin-4-yl)ethanamine).

Knowing that there was selection for a large variety of cycle 1 and cycle 2 building blocks, the common pharmacophore intersection product (**11c**, large dot) was chosen for off-DNA activity confirmation. For simplicity, the attachment point to DNA was substituted by an ethylamide. Given the larger variability observed for the selection output for both cycle 1 and cycle 2 residues, we chose one additional cycle 1 (isophthalic acid) and cycle 2 building block (2-(piperazin-1-yl)ethanamine)) and synthesized a 2 × 2 library for off-DNA biochemical activity confirmation (Scheme 1). This produced a sufficient number of off-DNA compounds to confirm activity of the chemotype and allowed for potential off-DNA preliminary SAR studies.

Chemistry

Assembly of the 2 × 2 library for off-DNA confirmation of the selected chemotype was accomplished by carboxylating commercially available 4-chlorothieno[3,2-*d*]pyrimidine (**12**, Scheme 1) to obtain carboxylic acid **13**. Treating **13** with oxalyl chloride, and quenching the intermediate acid chloride with ammonia in dioxane afforded the versatile 4-chlorothieno[3,2-*d*]pyrimidine-6-carboxamide intermediate **14**. The chloride on **14** was subsequently displaced with 4-(2-Boc-aminoethyl)piperidine or 4-(2-Boc-aminoethyl)piperazine to afford the Boc-protected precursors (**15a-b**). The Boc groups were removed by treatment with trifluoroacetic acid in CH_2Cl_2, and the resulting amines (**16a-b**) were reacted under

amide coupling conditions (HATU, DIEA) with (3-(ethylcarbamoyl)benzoic acid or 5-(ethylcarbamoyl)thiophene-2-carboxylic acid to afford **11a-d**. Most other analogs in this study were synthesized through similar transformations (see Supplemental Information).

SAR Studies

The four off-DNA synthesized representative compounds (Table 1, **11a-d**) were evaluated for their ability to inhibit the sirtuin mediated deacetylation of a minimal natural peptide substrate (Ac-RHKK^{Ac}W-NH_2)[34] in a biochemical assay with SIRT1, SIRT2 and SIRT3. The activity data was evaluated, in addition to physicochemical and calculated properties (solubility, CHI LogD,[35] tPSA, CLogP) to determine drug-like properties.

The representative common chemotype **11c** displayed excellent SIRT3 potency with an IC_{50} of 4 nM, confirming that the off-DNA chemotype was a functional inhibitor for SIRT3 and not merely a ligand with high affinity. It was also observed to have analogous potency against SIRT1 and SIRT2. Collectively, all the compounds in the 2 × 2 library (**11a-d**) were very potent pan inhibitors of SIRT1, SIRT2 and SIRT3. Replacement of the piperidine of **11c** with a piperazine (**11d**) only slightly reduced the potency against SIRT2 (≤ 2-fold) while reducing inhibition of SIRT1 and SIRT3 7-8 fold. The corresponding phenyl based analogs (**11a, 11b**) showed a similar trend. Comparing the effect of replacing the thiophene of **11c-d** with a phenyl (**11a-b**) revealed a general decrease in potency for SIRT1 and SIRT2 (2 fold). Analysis of the physiochemical properties of **11a-d** revealed that the more basic piperazines imparted a lowering of CLogP, LogD and a concurrent 10-fold improvement in aqueous solubility. The change from thiophene to benzene had little effect on physiochemical properties.

The off-DNA compounds (**11a-d**) represented a novel and highly potent new class of SIRT1/2/3 pan inhibitors. While the goal of identifying novel sirtuin inhibitor scaffolds was achieved, inhibitors **11a-d** tended to have suboptimal drug-like properties (MW, PSA, solubility and aromatic ring count) which limited their progression. To explore the possibility of improving the physiochemical properties of the

potent analog **11c**, the thieno[3,2-*d*]pyrimidine-6-carboxamide core was kept stationary and **11c** was truncated from the DNA tag end. The systematically truncated analogs were prepared (Supplemental Information) and evaluated in the SIRT1, SIRT2 and SIRT3 biochemical inhibition assays (Table 2).

Changing the ethylamide substituent on the thiophene to either a *tert*-butyl ester **17**, carboxylic acid **18** or hydrogen **19** resulted in only modest (ca. 2-fold) reductions of SIRT1, SIRT2 or SIRT3 potency, suggesting that the terminal ethylamide is not essential for activity. Encouraged by these results, we next evaluated the impact of removing the thiophene ring. Replacing the thiophene in **19**, with a *tert*-butyl carbamate (**15a**) resulted in a 3-4 fold reduction of SIRT1 and SIRT3 activity, while SIRT2 inhibition remained unchanged. When the thiophene in **19** was replaced with an acetamide (**20**), we observed more pronounced reductions in SIRT1 (18-fold), SIRT2 (3-fold) and SIRT3 (7-fold) activity. This trend continued with the removal of the acetamide in the amine analog **16a**, which was 5- to 15-fold less potent than **20**. Replacing the aminoethylpiperidine with a piperidine (**21**) dramatically reduced the sirtuin inhibitory activity to micromolar levels, and SIRT1/2/3 inhibitory activity was abolished in the severely truncated ethylamine **22** or chloride **14**. These results indicated that the thieno[3,2-*d*]pyrimidine-6-carboxamide core alone was not sufficient to inhibit SIRT1/2/3.

Of the truncated analogs presented, compound **20** exhibited the best balance of SIRT1/2/3 inhibitory potency (23 - 110 nM) and low molecular weight (MW = 347). To further optimize the potency, a larger compound set (Table 3) was prepared where variation of three areas was explored. 1) The effect of changing the piperidine to the more-polar piperazine (X = CH or N) ring system was evaluated. 2) The linker length (n) was varied to determine the optimal distance between the functional group and the thienopyrimidine core. 3) And the acetamide functionality on **20** was replaced with thioacetyl-, pivaloyl-, sulfonamide or pyrrolidine groups.

In general, the ethyl piperidines (X = CH, n = 2) were more potent inhibitors than the ethyl piperazines (X = N, n = 2), (compare **20** vs. **24**, **25** vs. **26**, **28** vs. **30**, **31** vs. **32**). However, for the pyrrolidine variants (**34** and **35**) the piperazine (X = N) analog displayed similar or greater potency on SIRT1, SIRT2 or SIRT3 versus the corresponding piperidine (X = CH) versions.

Linker length changes were evaluated on the acetamides (**20** and **23**), pivaloylamides (**27 - 29**), and the pyrrolidines (**33** and **34**). Taking the case of the pivaloylamides, the ethyl linker (**28**, n = 2) is slightly more potent than the longer propyl linker (**29**, n = 3), and the shorter methylene linker (**27**, n = 1) led to a dramatic decrease in SIRT1, SIRT2 and SIRT3 potency. This dramatic decrease in potency with a shorter (n = 1) linker length was broadly observed in other analogs (**23** and **33**).

Replacing the acetamide (**20** and **24**) with a thioamide (**25** and **26**) was well tolerated, resulting in modest improvements in potency. Changing the acetyl groups to the more lipophilic pivaloylamide or the polar sulfonamides was advantageous for sirtuin inhibition. Interestingly, the sulfonamide **31** which contains the optimal structural elements for inhibition (X = CH, n = 2) is a single digit nanomolar inhibitor of SIRT1, SIRT2 and SIRT3 and represents one of the most potent pan-inhibitors in the study. When evaluating the pyrrolidine analogs (**33 - 35**), the selectivity profile appears to slightly favor SIRT3 inhibition over SIRT1 and SIRT2. In general, there appears to be broad functional group tolerance in this region of the inhibitors (e.g. lipophilic, polar, basic, H-bond donor or acceptor groups are tolerated).

The SAR of the heteroaromatic thieno[3,2-*d*]pyrimidine core was also evaluated. Utilizing the potent pan inhibitor **28** as a comparator, a small series of heteroaromatic carboxamide cores were tested for their ability to inhibit SIRT1/2/3 (Table 4). Replacing the core of **28** (X = S) with furo[3,2-*d*]pyrimidine-6-carboxamide (**36**, X = O) resulted in 15- to 40-fold reductions in SIRT1/2/3 potency. To evaluate the pyrimidine portion of the heteroaromatic core, two thienopyridine carboxamide scaffolds were prepared. The first thienopyridine analog, where N3 (adjacent to the piperidine) was replaced with a CH (**37**, Y = CH) had modest reductions in SIRT1/2/3 inhibition (3- to 4-fold), whereas replacing N1 with a CH (**38**, Z = CH) resulted in more significant (30- to 63-fold) reductions in potency. To assess

the sensitivity of the unsubstituted position of the thiophene ring, a methyl was added at the 7-position (**39**) which reduced activity 4-12 fold across all three enzymes.

Lastly, the SAR of the carboxamide was also evaluated by making small adjustments at the 6-position of the thieno[3,2-*d*]pyrimidine core of **28** (Table 5). The N-methylcarboxamide (**41**) displayed a dramatic loss in SIRT2 activity, and no measurable SIRT1 or SIRT3 activity. Similarly, changing the carboxamide to a carboxylic acid (**40**) or complete removing of the carboxamide (**42**) resulted in no abolishing the SIRT1, SIRT2 and SIRT3 activity. These results indicate that the carboxamide is important for maintaining SIRT1/2/3 inhibition and it is likely involved in critical contacts with the protein. This strong connection between structural modification of the carboxamide group and SIRT inhibition is similar to the SAR that is observed with the carboxamide group of **4**.[17]

SIRT3 X-ray Structural Studies

There have been several reported crystal structures for the sirtuins[33, 36-39] including SIRT1, SIRT2, SIRT3 and SIRT5. The sirtuins have variable N- and C-terminal regions, and a conserved catalytic core containing two lobes; a large Rossmann lobe, and a smaller lobe with a structural zinc binding motif. Acetylated substrates bind in the cleft formed at the interface of the two lobes with the acetylated lysine projecting toward the nicotinamide riboside portion of NAD^+. A flexible loop, on the smaller lobe, closes down during the course of the deacetylation reaction to protect the imidate intermediate from solvent exposure.

Previously, we have reported the crystal structures of human SIRT3 (PDB code: 3GLS), substrate bound Ac-ACS2/SIRT3 (PDB code: 3GLR), the imidate reaction intermediate mimetic SIRT3-ACS2-$K_{s\text{-}ac}$-ADPR (PDB code: 3GLT) and the ternary carbaNAD/ACS2/SIRT3 (PDB code: 4FVT). In this study, the identified ELT hit (**11c**) and two of the most potent truncated pan SIRT1/2/3 inhibitors (**28** and **31**) were evaluated by X-ray crystallography in complex with human SIRT3 (Figure 4, S1-3). Crystals of SIRT3 and the inhibitors were obtained by co-crystallization with SIRT3(118-399). Crystals of SIRT3/**11c** (PDB code: 4JSR) and SIRT3/**31** (PDB code: 4JT9) diffracted to 1.70 and 2.25 Å,

respectively. However, for SIRT3/**28** the diffraction quality of the crystals was poor. Therefore **28** was soaked and exchanged into SIRT3/**31** crystals to achieve a suitable diffraction of 2.26 Å for SIRT3/**28** (PDB code: 4JT8).

DISCUSSION

Globally, the overall fold of the binary SIRT3/inhibitor structures is very similar to the previously reported structures of human SIRT3 (PDB codes: 3GLR, 3GLS, 3GLT, 3GLU, 4FVT). The Rossmann fold is highly superimposable, and there is domain closure upon binding to either substrates, cofactor intermediates[33, 37] or active-site targeting inhibitors (**11c**, **28**, **31**; this study). The largest divergence among the SIRT3 structures occurs at the flexible loop Ile154-Tyr175, which closes down on the nicotinamide C-pocket (Figure 4a).

The three SIRT1/2/3 pan inhibitors (**11c**, **28** and **31**) bind identically in the catalytic active site (RMS = 0.29 Å, Figure S2), occupying the nicotinamide C-pocket (Figures 4c, S3) and acetyl lysine substrate channel (Figures 4d, S3). Closer evaluation of the binding interactions of **11c** (Figures 4b-d) reveals that the carboxamide makes four hydrogen bonds with the protein surface, similar to the analogous nicotinamide portion of carba-NAD^+.[37] The 6-carboxamide carbonyl of **11c** accepts hydrogen bonds from protein backbone NH's of Ile230 and Asp231. One 6-carboxamide NH donates into the carboxylic acid on Asp231, while the other carboxamide NH hydrogen bonds to structural bridging water (W31), which is held in place by Ala146 and Ile154.

The nicotinamide of the SIRT3/ACS2/carba-NAD^+ complex makes very similar hydrogen bonding contacts to Ile154, Ala146, Ile230 and the neighboring structural water (Figures 5a-b). This recognition motif for the nicotinamide of NAD^+ is mimicked very well by the sirtuin inhibitors (**11c**, **28** and **31**) and explains the observed SAR in Table 5. As a result, a substantial reduction of sirtuin inhibitory activity is observed for compounds that lack the ability to make these critical hydrogen bonds in the nicotinamide C-pocket (**40**, R = CO_2H; **41**, R = CONHMe and **42**, R = H).

Moving toward the substrate channel, the thieno[3,2-*d*]pyrimidine aromatic core lines the top portion of the receptor pocket, along the hydrophobic zinc binding lobe. The thieno[3,2-*d*]pyrimidine π-stacks with the phenyl ring of Phe157 (Figures 4c-d) and the pyrimidine nitrogen (N1) is orientated to hydrogen bond with the Phe157 backbone resulting in an improvement in inhibitory activity (compare **28** vs. **38**). The other pyrimidine nitrogen (N3) is solvent exposed, allowing for hydrogen bonding with water, resulting in an interaction that produces only a small improvement in inhibitory activity (compare **28** vs. **37**). The slight loss of activity for **37** (compared to **28**) could also be explained by the presence of the CH twisting the neighboring piperidine slightly out of plane of the core.

The ethyl piperidine of **11c** adopts an extended conformation sitting along the top of a hydrophobic cleft under the small structural domain (defined by Tyr165, Phe180, Ile230, Ile291 and Phe294) while the arylamide is directed toward the N-acetyllysine substrate channel. The hydrophobic nature of this shelf explains why the lipophilic piperidines (**11a, 11c, 20, 28** and **31**) are more potent sirtuin inhibitors than the polar piperazine analogs (**11b, 11d, 24, 30** and **32**).

Further along the substrate channel, the aryl amide NH hydrogen bonds with Val292. In other substrate bound structures (3GLR and 4FVT), Val292 forms a hydrogen bond with the N-ε-acetyl lysine from the substrate (Figures 5a-b). For the SIRT1/2/3 inhibitors, a modest improvement in inhibition is observed with increasing acidity of the NH donor that interacts with Val292. For instance, comparing the SIRT1/2/3 inhibitory activity of the sulfonamide **25**, with acetamide **20** reveals an 8- to 28-fold improvement in potency. However, the lack of an available NH donor to interact with Val292, as exemplified by the pyrrolidine **34**, resulted in only modest changes in sirtuin inhibitory activity.

The X-ray structures also provided an explanation for the SAR observed for changes in the linker length (n). The ethyl linker (n = 2) for the piperidine (**20** & **28**) optimally align the amide NH to hydrogen bond with Val292, whereas the methylene analogs (n = 1, **23** & **27**) are too short to optimally make this interaction, resulting in a reduction of potency. The longer propylpiperidine (n = 3, **29**) is envisioned in twisting to accomidate this interaction, but at a slight loss of activity (1.5 - 3 fold).

Lastly, the distal ethylamide substituted on the 2-thiophene on **11c** makes a hydrogen bond with Glu296. This ethylamide, which was the point of attachment to the DNA linker in the ELT screen, extends out of the protein surface. Removing this portion had little effect on sirtuin inhibitory activity (see **19** vs. **11c**) given the sum of the other interactions the small molecule inhibitors make with in catalytic site.

The larger portion of the catalytic site, which is the space usually occupied by the ribofuranose to the adenine site of NAD^+, is still largely unoccupied in the SIRT3/**11c**, SIRT3/**28** and SIRT3/**31** structures, except for bulk water or crystallization medium. This space may be more efficiently exploited in future designs.

The residues that form the NAD^+ binding pocket are highly conserved between SIRT1/2/3, which likely explains why these compounds are pan inhibitors. Interestingly, several small molecule sirtuin inhibitors that have been described in the literature possess carboxamides, e.g. nicotinamide, **4** and benzamides (**7**) and structural modification of this group is strongly linked to changes in SIRT inhibition.

Recently, the ternary complex of the catalytic core of SIRT1(241-516), NAD^+ and a structural analog of EX527[17] (**43**, Figure 5c) was solved by X-ray crystallography[40]. Analysis of the ternary complex revealed that the carboxamide of **43** occupies the nicotinamide C-pocket with the indole projecting upward into a hydrophobic pocket between the flexible loop and a helix on the small lobe. Meanwhile, the nicotinamide of the cofactor swings out in an alternate inactive confirmation projecting toward the substrate channel.

Structural comparisons of the crystal structures of SIRT1/**43**/NAD^+ and SIRT3/**11c** (Figures 5c-d) reveal several similarities and differences in how these two classes of inhibitors bind. Globally, the Rossmann fold, NAD^+ cofactor binding channel and nicotinamide binding pockets are largely undisturbed. However, there is a shift of the SIRT1 small lobe onto the active site in the presence of **43**. Looking closer, the nicotinamide binding pockets, where the carboxamides of inhibitors **11c** and **43** bind, have identically conserved hydrogen bonding networks, explaining the sensitivity of the SAR of

the carboxamides in the EX527 analogs (**4** and **43**) and the inhibitors in this study. Interestingly, the orientation of the indole scaffold in **43** is 74 degrees normal to the thienopyrimidine scaffold of **11c** projecting into a narrow hydrophobic pocket, which could be an area of future exploitation to find additional classes of selective SIRT1 inhibitors.

Several regions on the small domain show differences in the two complexes. At the substrate channel entrance, the loop (Ile291-Leu298) in SIRT3/**11c** is more open to accommodate the distal thiophene carboxamide, whereas the identical loop (Ile411-Leu418) in SIRT1/**43**/NAD^+ closes downward to allow Phe414 to pi-stack with the backside of the nicotinamide of NAD^+. The analogous residue (Phe294) in SIRT3/**11c** is situated just above the N-ε-acetyl lysine binding site.

At the flexible loop region (Asp156-Pro174) of the SIRT3/**11c** complex, Phe157 pi-stacks with the thienopyrimdine core of **11c**, whereas in the SIRT1/**43**/NAD^+ complex, the same sequence (Asp272-Pro291) forms a helix and the analogous Phe273 side chain closes in to cap the hydrophobic cage for **43**. Additional shifts are observed for other hydrophobic residues on the small lobe of SIRT1/NAD^+/**43** complex (Tyr280, Phe297 and Phe413) which collapse to form the hydrophobic cage, whereas in SIRT3/**11c** the analogous residues (Tyr165, Phe180 and Phe293) form the upper hydrophobic shelf to accommodate the binding of **11c**.

The observed SAR is in strong agreement with the observed ligand interactions found in the SIRT3/**11c**, SIRT3/**28** and SIRT3/**31** crystal structures. Compounds **11c** and **28** were generally selective (XC_{50} > 10 μM) when profiled against a broad panel of kinases, nuclear receptors, ion channels, transporters and GPCRs. They do not inhibit hERG (**11c** and **28**; >50 μM, dofetilide binding) and are poor CYP inhibitors (**28**; 1A2, 2C19, 2D6 and 3A4 > 50 μM, 2C9 = 7.2 μM). Furthermore, compound **28** has a low LogD (2.73), high solubility (297 μM) and was stable in microsomal incubations (Human CL_{int} = 15.8 μL/min/mg, Mouse CL_{int} = 12.7 μL/min/mg).

CONCLUSION

A novel class of potent SIRT1/2/3 pan inhibitors was identified by utilizing encoded library technology to enrich for molecules that interact with SIRT3. Based on the analysis of the ELT sequencing data, the selected cycle 3 building block (thieno[3,2-*d*]pyrimidine-6-carboxamide) was a preferred core scaffold which was critical for the chemotype inhibitory function.

The initially prepared off-DNA library confirmed that compounds **11a-d** were very potent pan SIRT1/2/3 inhibitors. Reduction of molecular weight, to improve physiochemical properties of **11c**, resulted in the identification of the acetamide **20** as a good compromise of potency and reduced molecular weight. Further SAR showed that the thioacetyl **25**, *tert*-butyl-amide **28** and sulfonamide **31** were particularly potent pan inhibitors.

To better understand binding interactions, three pan inhibitors (**11c**, **28** and **31**) were crystallized with SIRT3. The thieno[3,2-*d*]pyrimidine-6-carboxamide inhibitors bind in the active site cleft, in between the large Rossmann fold and the small zinc binding domain occupying the nicotinamide C-pocket in addition to the substrate channel. Comparisons with previously described SIRT3 structures revealed similar protein folding, except for the flexible loop region where Phe157 makes a π-stacking interaction with the thienopyrimidine core. The carboxamide on the inhibitors, which is essential for activity, makes key hydrogen bonding interactions with residues in the nicotinamide binding pocket, similar to carba-NAD^+ and the recently described ternary complex of SIRT1/NAD^+/**43**.

The pan inhibitor **11c** and the truncated analogs **28** and **31**, represent a significant advance over currently available sirtuin inhibitors. Their binding mode, corroborated by X-ray crystallographic data, is in good agreement with the observed SAR. The potency of this class of inhibitors makes them valuable tools for understanding the biological effects of modulating the deacetylase activity of SIRT1, SIRT2 and SIRT3.

EXPERIMENTAL METHODS

Materials

Thioacetylated peptide (ACS2-$K_{s\text{-}Ac}$: TRSG$K_{thioacetyl}$VMRRLLR) which has the same sequence as the ACS2K_{ac} peptide with the acetyl lysine replaced with thioacetyl lysine using Fmoc-Lys($CSCH_3$)-OH was prepared as previously described.[33]

ELT Affinity Selection

Selections were carried out by capturing 2 μg of Flag-hSIRT3(118-399)-SBP on streptavidin matrix tips (Phynexus) in the presence of 1) no β-NAD/no peptide substrate, 2) 100 μM β-NAD (Sigma), or 3) 20 μM TRSG$K_{thioacetyl}$VMRRLLR for three rounds. A no target control selection with buffer was carried out concurrently in the absence of SIRT3 protein.

Streptavidin tips were pre-washed in selection buffer: 50 mM Tris (pH 7.5), 150 mM NaCl, 0.1% Tween-20, and 0.1 mg/mL sheared salmon sperm DNA (sssDNA, Ambion), 0.1 mg/mL BSA (Ambion) and 5 mM β-mercaptoethanol (BME). In the first round of selection, 2 μg of Flag-hSIRT3(118-399)-SBP protein was immobilized on pre-washed tips in the presence of 1) no β-NAD/no peptide substrate, 2) 100 μM β-NAD or 3) 20 μM thioacetylated peptide. The tips were washed two times with buffer containing the corresponding cofactor and substrate when necessary. Pooled ELT libraries (5 nmoles) were passed over the immobilized SIRT3 in the presence of the corresponding cofactor and substrate for 1 hour at room temperature. The tips were washed 8 times with selection buffer containing the corresponding cofactor and substrate and two times with BSA free selection buffer containing the corresponding cofactor and substrate. Bound molecules were heat eluted by passing BSA free selection buffer containing no cofactors and substrates over the tip at 72 °C for 10 minutes. The cooled heat elution was post-cleared twice by passing the elution over streptavidin tips for 15 min to remove any denatured SIRT3 and matrix binders. Fresh BSA and sssDNA were added to all samples and corresponding cofactor and substrate was added to the elutions as needed. Round 2 was performed as described for Round 1 using freshly immobilized SIRT3 on streptavidin tips in the presence of

corresponding cofactor and substrate and post-cleared Round 1 output. Round 3 was performed as described for Round 1 using freshly immobilized SIRT3 on streptavidin tips in the presence of corresponding cofactor and substrate and post-cleared Round 2 output with the exceptions that the last two washes and elution were with BSA-free and sssDNA-free selection buffer and the round 3 output was not post-cleared. Quantitative PCR was used to quantitate the outputs from each round of selection. The round 3 output was sequenced using an Illumina sequencing platform.

Protein Cloning, Expression, and Purification

Human SIRT3-(118–399) was cloned into a proprietary modified pET21b vector (Viva Biotech). The protein was expressed in E. coli BL21-Gold(DE3) cells (Stratagene) as an N-terminal fusion to a hexahistidine affinity tag with an integrated TEV protease site. A single colony was inoculated in LB media containing 100 μg/ml ampicillin at 37 °C, swirled at 250 rpm until the A_{600} reached 0.3. The culture was then cooled to 18 °C, swirled at 250 rpm until the A_{600} reached 0.6–0.8. 1-(2-isopropylthio)-β-D-galactopyranoside (IPGT) was added to a final concentration of 0.3 mM, and expression was continued at 18 °C, swirled at 160 rpm overnight. Cells were collected by centrifugation, and the pellet was re-suspended in lysis buffer (200 mM NaCl, 5% glycerol, 5 mM 2-mercaptoethanol, and 25 mM HEPES-NaOH, pH 7.5) and sonicated to break the cells. The supernatant was separated from the cell debris by centrifugation at 10,000 × g for 40 min at 4 °C and loaded onto a Ni-NTA column (Qiagen) that was equilibrated with a buffer containing 200 mM NaCl, 5% glycerol, 5 mM 2-mercaptoethanol, 20 mM imidazole, and 25 mM HEPES-NaOH, pH 7.5. The column was washed with 5 column volumes of a buffer containing 200 mM NaCl, 5% glycerol, 5 mM 2-mercaptoethanol, 50 mM imidazole, and 25 mM HEPES-NaOH, pH 7.5, then eluted with a buffer containing 200 mM NaCl, 5% glycerol, 5 mM 2-mercaptoethanol, 250 mM imidazole, and 25 mM HEPES-NaOH, pH 7.5. The eluted protein was dialyzed in lysis buffer and digested with TEV protease (Invitrogen) at 4 °C overnight to remove the N-terminal His tag. The protein was loaded on a second Ni-NTA column equilibrated with lysis buffer. The untagged protein was eluted with a buffer containing 200 mM NaCl, 5% glycerol, 5 mM 2-

mercaptoethanol, 5 mM imidazole, and 25 mM HEPES-NaOH, pH 7.5. The purified protein was dialyzed against a buffer containing 200 mM NaCl, 5 mM 2-mercaptoethanol, and 20 mM Tris-HCl, pH 8.0, and concentrated. The protein was further purified by elution with dialyzing buffer over a S200 column (GE Healthcare) to 95% purity as assessed by SDS-PAGE analysis stained by Coomassie Brilliant Blue R-250, and concentrated to 10–15 mg/ml in the dialyzing buffer.

SIRT1, SIRT2 and SIRT3 Biochemical assays

Deacetylation of a Trp 5-mer peptide (Ac-RHKK$_{Ac}$W-NH, Biopeptide, San Diego, CA) by His-SIRT1(1-747), His-SIRT2(1-389) and His-SIRT3(102-399) was measured by a discontinuous OAADPr Mass Spec assay which measures OAADPr (2'-O-acetyl-ADP-ribose) production. All assays were performed at room temperature in reaction buffer (50 mM HEPES, pH 7.5, 150 mM NaCl, 1 mM DTT, 0.05% BSA). Test compounds (1 μL in DMSO) were pre-incubated with either SIRT1 (5 nM), SIRT2 (10 nM) or SIRT3 (5 nM) in reaction buffer (50 μL) for 20 minutes. For IC_{50} determination, Trp 5-mer peptide was added at K_M conditions (2 μM for SIRT1, 10 μM for SIRT2 or 2.2 μM for SIRT3) along with NAD at K_M (80 μM for SIRT1, 50 μM for SIRT2 and 130 μM SIRT3) for a final volume of 100 μL. The reaction was quenched after 30 minutes with 10 μL of stop buffer (50 mM Nicotinamide in 10% formic acid) to give a final concentration of 0.9% formic acid and 4.5 mM nicotinamide. To prepare the assays for analysis, 20 μL of reaction volume was mixed in 80 μL of 50:50 acetonitrile/methanol mixture. The plates were analyzed on an Agilent RapidFire 200 High-Throughput Mass Spectrometry System (Agilent, Wakefield) coupled to an AB Sciex API 4000 mass spectrometer fitted with an electrospray ionization source in negative MRM mode monitoring the transition 600.1/345.9 for the parent/daughter ion under low resolution conditions. Peak data was integrated using RapidFire Integrator software (Agilent, Santa Clara, CA).

Crystallization and Structural Determination of SIRT3 Complex

SIRT3/**31** and SIRT3/**11c** crystals were obtained by hanging drop vapor diffusion method at 18 °C. The drop was composed of 1 μl of protein/compound mixture and 1 μl crystallization buffer. For SIRT3/**31** the crystallization condition was 0.1 M HEPES pH 7.5 20% w/v PEG 8000. The crystallization buffer for SIRT3/**11c** was 0.1M Tris pH 8.0, 20% PEG 4000 or 20% PEG 6000. The SIRT3/**31** crystals were soaked for 4 h in 10 mM **28** in crystallization buffer to obtain SIRT3/**28** crystals.

The SIRT3/**31** and SIRT3/**11c** crystals were cryo-protected in mother liquor, which contained 20% glycerol before being flash-frozen in liquid nitrogen. The SIRT3/**31** crystals soaked in **28** were cryo-protected in mother liquor, which contained 20% glycerol and 10 mM **28**. The diffraction data was collected at Shanghai Synchrotron Radiation Facility (SSRF) beamline workstations BL17U1 and APS 21-ID-D and processed using the Xia2[41] or HKL2000[42] programs. The structures were solved by molecular replacement with Phaser[43] using the substrate bound ACS2/SIRT3 structure (PDB code: 3GLR) as a search model. Iterative structure refinement and model building were performed between Refmac[44] in the CCP4 suite[45] and Coot[46]. Detailed information regarding the diffraction data, refinement, and structure statistics is listed in the Supporting Information. All the parameters for each diffraction data set were reprocessed using Mosflm[47] and Scala[48] and the refinement statistics were obtained from Refmac[44] in the CCP4 suite[45].

Synthetic Methods

Unless otherwise noted, all reagents and solvents were obtained from commercial suppliers and used without further purification. Purities of all assayed compounds were determined by analytical HPLC using the area percentage method on the UV trace recorded at a wavelength of 254 nm, and were found to have ≥ 95% purity unless otherwise specified. Analytical HPLC was performed on an Agilent 1100 Series HPLC equipped with a 3.5 μm Eclipse XDB-C18 (4.6 mm × 100 mm) column with the following conditions: CH_3CN/H_2O, modified with 0.1% formic acid mobile phase. Gradient elution: 5% CH_3CN hold (2 min), 5% to 95% CH_3CN gradient (11 min), 95% to 5% CH_3CN gradient (0.3 min), 5% CH_3CN

hold (2.7 min), 15 min. total run time with a flow rate of 0.8 ml/min. Low-resolution Mass spectroscopy (LRMS) was performed on an Agilent 1100 Series LC/MSD single quadrupole in electrospray ionization. High Resolution Mass Spec (HRMS) was completed on a Waters qTOF Premiere Mass Spectrometer operating in W mode positive ionization with a resolving power of approximately 15,000. Flow injection was completed using a Waters nano-acquity LC. HRMS acceptable error is 3 mDa or 5 ppm, although most analyses are observed within 0.5 mDa with isotope fits in good agreement with the proposed structures. Nuclear magnetic resonance (NMR) spectra were recorded on a Bruker AVANCE-III 300 or 400 MHz instrument referenced with the appropriate internal standard (TMS: δ = 0 ppm). Flash column chromatography was performed on silica gel, particle size 60 Å, mesh of 230−400 (Merck) under standard techniques. All microwave reactions were conducted on a Biotage Initiator Microwave Synthesizer.

4-Chlorothieno[3,2-*d*]pyrimidine-6-carboxylic acid (13). To a stirring solution of 2,2,6,6-tetramethylpiperidine (1.484 mL, 8.79 mmol) in anhydrous THF (15 mL) at 0 °C under nitrogen was added 2.5 M BuLi in hexanes (3.52 mL, 8.79 mmol) dropwise. The reaction mixture was stirred at 0 °C for 30 minutes, then the mixture was added to a solution of 4-chlorothieno[3,2-*d*]pyrimidine (1.00 g, 5.86 mmol) in anhydrous THF (15 mL) at -78 °C dropwise over a period of 30 minutes. The reaction was stirred at -78 °C for 1 hour, then to the reaction was added dry ice (2.58 g, 58.6 mmol). The reaction was allowed to warm up to room temperature over a period of 2 hours. The reaction was diluted with EtOAc (100 mL) and washed with 0.1 M HCl. The organic layer was dried over $MgSO_4$ and evaporated to dryness to obtain 4-chlorothieno[3,2-*d*]pyrimidine-6-carboxylic acid (1.1 g, 83%). ^{1}H NMR (DMSO-d_6) δ 14.5 (br s, 1H), 9.16 (s, 1H), 8.27 (s, 1H). LRMS (ESI) 215.0 $[M + H]^+$.

4-Chlorothieno[3,2-*d*]pyrimidine-6-carboxamide (14). To a solution of oxalyl chloride (4.17 mL, 47 mmol) in anhydrous dichloromethane (50 mL) at 0 °C under nitrogen was added DMF (0.8 mL). The solution was stirred at 0 °C for 30 minutes, and then a suspension of 4-chlorothieno[3,2-*d*]pyrimidine-6-carboxylic acid (5.04 grams, 23.5 mmol) in dichloromethane (50 mL) was added dropwise over 10 minutes at 0 °C. The reaction mixture was heated to reflux for 3.5 hours and concentrated to dryness.

The crude acid chloride was dissolved in dioxane (80 mL) and 182 mL (91 mmol) of a solution of 0.5 M ammonia in dioxane was added dropwise over 10 min at 0 °C. The reaction mixture was stirred at 0 °C for 30 min, warmed to room temperature, diluted with water (150 mL) and extracted with CH_2Cl_2 (3x). The combined organic layers were washed with water (2x), dilute aq. $NaHCO_3$, brine and concentrated to dryness. The product was recrystallized from CH_3CN to obtain 842 mg of 4-chlorothieno[3,2-*d*]pyrimidine-6-carboxamide. The mother liquor was concentrated to obtain a second crop (1499 mg) and a third crop (259 mg), of 4-chlorothieno[3,2-*d*]pyrimidine-6-carboxamide (2.6 g, 52%). ^{1}H NMR (DMSO-d_6) δ 9.11 (s, 1H), 8.62 (br s, 1H), 8.35 (s, 1H), 8.15 (br s, 1H). ^{13}C NMR (DMSO-d_6) δ 161.53, 161.21, 154.75 (CH), 154.13, 150.77, 131.47, 124.80 (CH). LRMS (ESI) 214.0 $[M + H]^+$.

***tert*-Butyl (2-(1-(6-carbamoylthieno[3,2-*d*]pyrimidin-4-yl)piperidin-4-yl)ethyl)carbamate (15a).** A solution of 4-chlorothieno[3,2-*d*]pyrimidine-6-carboxamide (1.30 g, 6.08 mmol), *tert*-butyl (2-(piperidin-4-yl)ethyl)carbamate (1.39 g, 6.08 mmol) and DIEA (1.05 mL, 6.08 mmol) in CH_3CN (80 mL) was heated at reflux for 1 hour. The reaction mixture was cooled to room temperature and concentrated to dryness. The residue was suspended in MeOH (10 mL) then water (90 mL) was added. The mixture was sonicated and the precipitate was collected by filtration, washed with water and dried under high vacuum to obtain *tert*-Butyl (2-(1-(6-carbamoylthieno[3,2-*d*]pyrimidin-4-yl)piperidin-4-yl)ethyl)carbamate (2.23 g, 90%). ^{1}H NMR (DMSO-d_6) δ 8.48 (s, 1H), 8.40 (br s, 1H), 8.03 (s, 1H), 7.87 (br s, 1H), 6.81 (t, 1H), 4.69 (d, 2H), 3.16 (t, 2H), 2.976 (q, 2H), 1.83 (d, 2H), 1.66 (br, 1H), 1.37 (s, 9H), 1.34 (m, 2H), 1.16 (m, 2H). LRMS (ESI) 406.1 $[M + H]^+$. HRMS (m/z): $[M + H]^+$ calc for $C_{19}H_{28}N_5O_3S$, 406.1913; found, 406.1915.

***tert*-Butyl (2-(4-(6-carbamoylthieno[3,2-*d*]pyrimidin-4-yl)piperazin-1-yl)ethyl)carbamate (15b).** A solution of 4-chlorothieno[3,2-*d*]pyrimidine-6-carboxamide (250 mg, 1.17 mmol), DIEA (245 µL, 1.40 mmol) and *tert*-butyl (2-(piperazin-1-yl)ethyl)carbamate (332 mg, 1.40 mmol) in CH_3CN (15 mL) was heated at 60 °C for 18 hours. The reaction mixture was cooled to room temperature and filtered to collect the product as a solid. The solid was washed with CH_3CN (2 x 10 mL) and dried to obtain *tert*-butyl (2-(4-(6-carbamoylthieno[3,2-*d*]pyrimidin-4-yl)piperazin-1-yl)ethyl)carbamate as a white solid

(440 mg, 93% yield). ^{1}H NMR (DMSO-d_6) δ 8.51 (s, 1H), 8.41 (br s, 1H), 8.05 (s, 1H), 7.88 (br s, 1H), 6.71 (t, 1H), 3.92 (m, 4H), 3.08 (q, 2H), 2.55 (m, 4H), 2.38 (t, 2H), 1.38 (s, 9H). LRMS (ESI): 407.2 [M + H]$^+$. HRMS (m/z): [M + H]$^+$ calc for $C_{18}H_{27}N_6O_3S$, 407.1865; found, 407.1866.

4-(4-(2-Aminoethyl)piperidin-1-yl)thieno[3,2-*d*]pyrimidine-6-carboxamide (16a). To a solution of *tert*-Butyl (2-(1-(6-carbamoylthieno[3,2-*d*]pyrimidin-4-yl)piperidin-4-yl)ethyl)carbamate (**15a**) (840 mg, 2.07 mmol) in CH_2Cl_2 (40 mL) was added Trifluoroacetic acid (10 mL). The reaction mixture was stirred for 72 hours, concentrated to dryness and chased with CH_2Cl_2 (2x). The residue was diluted with MeOH, then a solution of 1.25 M HCl in MeOH (2 mL) was added. To the resulting oil was added diethyl ether (15 mL) and pentane (5 mL). The solution was sonicated to produce solid which was isolated by decantation, and dried under vacuum to obtain 4-(4-(2-aminoethyl)piperidin-1-yl)thieno[3,2-*d*]pyrimidine-6-carboxamide as the hydrochloride salt (1.09 g) ^{1}H NMR (DMSO-d_6) δ 8.65 (s, 1H), 8.57 (br s, 1H), 8.08 (s, 1H), 7.987 (br s, 1H), 7.75 (br, 3H), 4.76 (d, 2H), 3.29 (t, 2H), 2.85 (m, 2H), 1.89 (d, 2H), 1.79 (s, 1H), 1.50 (m, 2H), 1.23 (m, 2H). LRMS (ESI): 306.1 [M + H]$^+$. HRMS (m/z): [M + H]$^+$ calc for $C_{14}H_{20}N_5OS$, 306.1389; found, 306.1389.

4-(4-(2-Aminoethyl)piperazin-1-yl)thieno[3,2-*d*]pyrimidine-6-carboxamide (16b). A solution of *tert*-butyl (2-(4-(6-carbamoylthieno[3,2-*d*]pyrimidin-4-yl)piperazin-1-yl)ethyl)carbamate (**15b**) (440 mg, 2.46 mmol) was stirred with 25% TFA in CH_2Cl_2 (8 mL) for 6 hours. The solution was concentrated to dryness and triturated with a mixture of diethyl ether and pentane mixture to obtain solid 4-(4-(2-aminoethyl)piperazin-1-yl)thieno[3,2-*d*]pyrimidine-6-carboxamide as a tan solid as the bis-TFA salt (844 mg, 64%). ^{1}H NMR (DMSO-d_6) δ 8.68 (s, 1H), 8.53 (br s, 1H), 8.13 (s, 1H), 7.97 (br s, 4H), 4.14 (br, 4H), 3.1-3.4 (m, 8H). LRMS (ESI): 307.2 [M + H]$^+$. HRMS (m/z): [M + H]$^+$ calc for $C_{13}H_{19}N_6OS$, 307.1341; found, 307.1341.

Methyl 5-(ethylcarbamoyl)thiophene-2-carboxylate. To a solution of 5-(methoxycarbonyl)thiophene-2-carboxylic acid (500 mg, 2.68 mmol) and HATU (1.23g, 3.23 mmol) in DMF (10 mL) was added DIEA (1.16 mL, 6.70 mmol). The reaction mixture was stirred at room temperature for 10 min, then ethylamine hydrochloride (219 mg 2.68 mmol) was added as a solid. The

reaction mixture was stirred for 7 h, and another batch of ethylamine hydrochloride (219 mg 2.68 mmol) and DIEA (1.16 mL, 6.70 mmol) was added and stirring was continued for a total of 24 h. To the reaction mixture was added sat. $NaHCO_3$ (30 mL) and water (50mL). The precipitated product was collect by filtration, and washed with water to obtain methyl 5-(ethylcarbamoyl)thiophene-2-carboxylate as a tan solid (555 mg, 97%). ^{1}H NMR (DMSO-d_6) δ 8.76 (t, 1H), 7.79 (d, 1H), 7.75 (d, 1H), 3.84 (s, 3H), 3.25 (m,2H), 1.12 (t, 3H). LRMS (ESI): 214.1 $[M + H]^+$.

5-(Ethylcarbamoyl)thiophene-2-carboxylic acid. To a solution of methyl 5-(ethylcarbamoyl)thiophene-2-carboxylate (555 mg, 2.60 mmol) in THF (5 mL) was added a solution of LiOH (124 mg, 5.18 mmol) in water (5 mL). The reaction mixture was stirred at room temperature for 72 h, concentrated to dryness, dissolved in water, and acidified with conc. HCl to pH =1. The precipitate was collected by filtration, washed with water and dried under vacuum to obtain 5-(ethylcarbamoyl)thiophene-2-carboxylic acid as an off white solid. (221 mg, 43%). ^{1}H NMR (DMSO-d_6) δ 13.40 (s, 1H), 8.71 (t, 1H), 7.71 (d, 1H), 7.68 (d, 1H), 3.26 (m, 2H), 1.12 (t, 3H). LRMS (ESI): 200.1 $[M + H]^+$.

Methyl 3-(ethylcarbamoyl)benzoate. A solution of 3-(methoxycarbonyl)benzoic acid (1.0 g, 5.55 mmol), HATU (2.53g, 6.65 mmol), DIEA (1.44 mL, 8.31 mmol) in DMF (15 mL) was stirred at room temperature for 10 min, then ethylamine (70% in water, 8.84 mL) was added and the reaction mixture was stirred at room temperature for 18 hours. The mixture was diluted with ethyl acetate and the organic layer was washed with sat. $NaHCO_3$, water (3 x), dried (Na_2SO_4), concentrated and chased with methanol to obtain methyl 3-(ethylcarbamoyl)benzoate as an orange oil (1.20 g) which was used without further purification in the next step.

3-(Ethylcarbamoyl)benzoic acid. To a solution of methyl 3-(ethylcarbamoyl)benzoate (1.20 g) in methanol (50 mL) was added LiOH (666mg, 27.8 mmol) in water (10 mL). The reaction mixture was stirred at room temperature for 72 h, concentrated to dryness, dissolved in water, and acidified with conc. HCl to pH =1-2. The precipitate was collected by filtration, washed with water and dried to obtain 3-(ethylcarbamoyl)benzoic acid (793 mg, 74% after 2-steps). ^{1}H NMR (DMSO-d_6) δ 13.17 (s, 1H), 8.67

(t, 1H), 8.42 (m, 1H), 8.07 (m, 1H), 7.59 (t, 1H), 3.30 (m, 2H), 1.13 (t, 3H). LRMS (ESI): 194.1 [M + H]$^+$.

General procedure for the synthesis of 11a-11d. Step 1) To a solution of appropriate Boc protected amine (0.166 mmol) in dichloromethane (6 mL) was added TFA (0.309 mL, 4.0 mmol). The reaction mixture was stirred for 1 h. The excess TFA and solvents were evaporated, then the residue was azeotroped with DCM (2 x). The resulting amine was carried to the next step as is. Step 2) To a mixture of desired carboxylic acid (0.200 mmol) and HATU (76 mg, 0.200 mmol) in DMF (3 mL) was added DIEA (0.175 mL, 1.0 mmol). The reaction mixture was stirred for 10 min, then the appropriate amine from step 1 was added. The reaction mixtures were allowed to stir at room temperature overnight, and the products were purified by prep HPLC.

***N*^{1}-(2-(1-(6-carbamoylthieno[3,2-*d*]pyrimidin-4-yl)piperidin-4-yl)ethyl)-*N*^{3}-ethylisophthalamide (11a).** The title compound was synthesized according to the general procedure using *tert*-butyl (2-(1-(6-carbamoylthieno[3,2-*d*]pyrimidin-4-yl)piperidin-4-yl)ethyl)carbamate (67.2 mg, 0.166 mmol) and 3-(ethylcarbamoyl)benzoic acid (40 mg, 0.207 mmol) to afford **11a** (90 mg, 77%). ^{1}H NMR (DMSO-d_6) δ 8.57 (m, 2H), 8.48 (s, 1H), 8.40 (br, 1H), 8.29 (m, 1H), 8.04 (s, 1H), 7.95 (m, 2H), 7.86 (br, 1H), 7.54 (t, 1H), 4.71 (m, 2H), 3.25-3.40 (m, 5H) 3.1-3.25 (m, 2H), 1.91 (m, 2H), 1.75 (m, 1H), 1.51 (q, 2H), 1.2-1.3 (m, 2H), 1.13 (t, 3H). LRMS (ESI): 481.35 [M + H]$^+$. HRMS (m/z): [M + H]$^+$ calc for $C_{24}H_{29}N_6O_3S$, 481.2022; found, 481.2021.

***N*^{1}-(2-(4-(6-carbamoylthieno[3,2-*d*]pyrimidin-4-yl)piperazin-1-yl)ethyl)-*N*^{3}-ethylisophthalamide (11b).** The title compound was synthesized according to the general procedure using *tert*-butyl (2-(4-(6-carbamoylthieno[3,2-*d*]pyrimidin-4-yl)piperazin-1-yl)ethyl)carbamate (67.3 mg, 0.161 mmol) and 3-(ethylcarbamoyl)benzoic acid (40 mg, 0.207 mmol) to afford **11b** (95 mg, 86%). ^{1}H NMR (DMSO-d_6) δ 8.57 (m, 2H), 8.52 (s, 1H), 8.41 (br, 1H), 8.29 (m, 1H), 8.05 (s, 1H), 7.95 (dd, 2H), 7.87 (br, 1H), 7.55 (t, 1H), 3.95 (m, 4H), 3.45 (q, 2H), 3.30 (m, 2H), 2.63 (m, 4H), 2.54 (m, 2H), 1.13 (t, 3H). LRMS (ESI): 482.30 [M + H]$^+$. HRMS (m/z): [M + H]$^+$ calc for $C_{23}H_{28}N_7O_3S$, 482.1974; found, 482.1974.

N^2-(2-(1-(6-carbamoylthieno[3,2-*d*]pyrimidin-4-yl)piperidin-4-yl)ethyl)-N^5-ethylthiophene-2,5-dicarboxamide (11c). The title compound was synthesized according to the general procedure using *tert*-butyl (2-(1-(6-carbamoylthieno[3,2-*d*]pyrimidin-4-yl)piperidin-4-yl)ethyl)carbamate (65.1 mg, 0.161 mmol) and 5-[(ethylamino)carbonyl]-2-thiophenecarboxylic acid (40 mg, 0.201 mmol) to afford **11c** (70 mg, 68%). ^{1}H NMR (DMSO-d_6) δ 8.67 (s, 1H), 8.56-8.62 (m, 3H), 8.06 (s, 1H), 8.00 (br, 1H), 7.68 (m, 2H), 4.76 (m, 2H), 3.21-3.37 (m, 6H), 1.95 (m, 2H), 1.76 (m, 1H), 1.49 (m, 2H), 1.25 (m, 2H), 1.11 (t, 3H). LRMS (ESI): 487.26 $[M + H]^+$. HRMS (m/z): $[M + H]^+$ calc for $C_{22}H_{27}N_6O_3S_2$, 487.1586; found, 482.1586.

N^2-(2-(4-(6-carbamoylthieno[3,2-*d*]pyrimidin-4-yl)piperazin-1-yl)ethyl)-N^5-ethylthiophene-2,5-dicarboxamide (11d). The title compound was synthesized according to the general procedure using *tert*-butyl (2-(4-(6-carbamoylthieno[3,2-*d*]pyrimidin-4-yl)piperazin-1-yl)ethyl)carbamate (65.3 mg, 0.161 mmol) and 5-[(ethylamino)carbonyl]-2-thiophenecarboxylic acid (40 mg, 0.201 mmol) to afford **11d** (90 mg, 94%). ^{1}H NMR (DMSO-d_6) δ 8.60 (m, 2H), 8.51 (s, 1H), 8.41 (br, 1H), 8.05 (s, 1H), 7.87 (br, 1H), 7.68 (s, 2H), 3.94 (m, 4H), 3.40 (q, 2H), 3.25 (m, 2H), 2.61 (m, 4H), 2.53 (m, 2H), 1.11 (t, 3H). LRMS (ESI): 488.15 $[M + H]^+$. HRMS (m/z): $[M + H]^+$ calc for $C_{21}H_{26}N_7O_3S_2$, 488.1539; found, 488.1540.

ANCILLARY INFORMATION

Supporting Information

X-ray diffraction and refinement parameters, view of the superposition of SIRT3/**11c**, SIRT3/**28** and SIRT3/**31,** binding site views of SIRT3/**28** and SIRT3/**31**, a view of the orientation of Phe157 in SIRT3 structures, and the synthetic details for compounds **17 – 42**. This material is available free of charge via the Internet at http://pubs.acs.org.

Accession Codes

The atomic coordinates and experimental data for SIRT3/**11c** (PDB code: 4JSR), SIRT3/**28** (PDB code: 4JT8), and SIRT3/**31** (PDB code: 4JT9) have been deposited into the RCSB Protein Data Bank (www.rcsb.org).

Corresponding Authors

For J.S.D.: phone, (508)-934-6975; e-mail: jdisch92@gmail.com. For G.E.: phone, (781)-795-4423; fax, (781)-795-4496; e-mail, ghotas.x.evindar@gsk.com.

Acknowledgements

The authors thank Matthew Lochansky for HRMS analysis and Andrew Haser for Microsomal Stability results. We are grateful for protein production and X-ray diffraction data collection by Dongming Qian, Fan Jiang, Yu Xia, Wentao Wei, and Jianhua Cai at Viva Biotech Ltd. Lastly, the authors thank Meidy Lontoh for compound plating and logistics, in addition to Andrew Maynard and Aaron Miller for modeling support.

Abbreviations Used

SIRT, sirtuin; ELT, Encoded Library Technology; NAD^+, nicotinamide adenine dinucleotide; SAR, structure activity relationship; ACS2, acetyl-CoA synthetase 2; ADPR, Adenosine Diphosphate Ribose; HATU, (O-(7-azabenzotriazol-1-yl)-*N,N,N′,N′*-tetramethyluronium hexafluorophosphate); DIEA, Diisopropylethylamine.

REFERENCES

1. Bauer, J. A.; Ungvari, Z.; Minor, R. K.; Le Couteur, D. G.; de Cabo, R., Are Sirtuins Viable Targets for Improving Healthspan and Lifespan? *Nat. Rev. Drug Disc.* **2012,** *11* (6), 443-461.

2. Finkel, T.; Deng, C. X.; Mostoslavsky, R., Recent progress in the biology and physiology of sirtuins. *Nature* **2009,** *460* (7255), 587-591.

3. Blum, C. A.; Ellis, J. L.; Loh, C.; Ng, P. Y.; Perni, R. B.; Stein, R., SIRT1 Modulation as a Novel Approach to the Treatment of Diseases of Aging. *J. Med. Chem.* **2011,** *54* (2), 417-432.

4. Banks, A. S.; Kon, N.; Knight, C.; Matsumoto, M.; Gutierrez-Juarez, R.; Rossetti, L.; Gu, W.; Accili, D., SirT1 gain of function increases energy efficiency and prevents diabetes in mice. *Cell Metab.* **2008,** *8* (4), 333-341.

5. Peck, B.; Chen, C.-Y.; Ho, K.-K.; P., D. F.; Myatt, S. S.; Coombes, R. C.; Fuchter, M. J.; Hsiao, C.-D.; Lam, E. W.-F., SIRT Inhibitors Induce Cell Death and p53 Acetylation through Targetting Both SIRT1 and SIRT2. *Mol. Cancer Ther.* **2010,** *9* (4), 844-855.

6. Wang, R. H.; Sengupta, K.; Li, C.; Kim, H. S.; Cao, L.; Xiao, C.; Kim, S.; Xu, X.; Zheng, Y.; Chilton, B.; Jia, R.; Zheng, Z. M.; Appella, E.; Wang, X. W.; Ried, T.; Deng, C. X., Impaired DNA damage response, genome instability, and tumorigenesis in SIRT1 mutant mice. *Cancer Cell* **2008,** *14* (4), 312-323.

7. Liu, L.; Arun, A.; Ellis, L.; Peritore, C.; Donmez, G., Sirtuin 2 (SIRT2) enhances 1-methyl-4-phenyl-1,2,3,6-tetrahydropyridine (MPTP)-induced nigrostriatal damage via deacetylating forkhead box O3a (Foxo3a) and activating Bim protein. *J. Biol. Chem.* **2012,** *287* (39), 32307-32311.

8. Tang, B. L., Sirt1's Complex Roles in Neuroprotection. *Cell. Mol. Neurobiol.* **2009,** *29* (8), 1093-1103.

9. Outeiro, T. F.; Kontopoulos, E.; Altmann, S. M.; Kufareva, I.; Strathearn, K. E.; Amore, A. M.; Volk, C. B.; Maxwell, M. M.; Rochet, J.-C.; McLean, P. J.; Young, A. B.; Abagyan, R.; Feany, M. B.; Hyman, B. T.; Kazantsev, A. G., Sirtuin 2 Inhibitors Rescue α-Synuclein-Mediated Toxicity in Models of Parkinson's Disease. *Science* **2007,** *317* (5837), 516-519.

10. Yoshizaki, T.; Milne, J. C.; Imamura, T.; Schenk, S.; Sonoda, N.; Babendure, J. L.; Lu, J. C.; Smith, J. J.; Jirousek, M. R.; Olefsky, J. M., SIRT1 exerts anti-inflammatory effects and improves insulin sensitivity in adipocytes. *Mol. Cell. Biol.* **2009,** *29* (5), 1363-1374.

11. Yoshizaki, T.; Schenk, S.; Imamura, T.; Babendure, J. L.; Sonoda, N.; Bae, E. J.; Oh, D.; Lu, M.; Milne, J. C.; Westphal, C.; Bandyopadhyay, G.; Olefsky, J. M., SIRT1 Inhibits Inflammatory Pathways in Macrophages and Modulates Insulin Sensitivity. *Am. J. Physiol.: Endocrinol. Metab.* **2010,** *298* (3), E419-E428.

12. Narayan, N.; Lee, I. H.; Borenstein, R.; Sun, J.; Wong, R.; Tong, G.; Fergusson, M. M.; Liu, J.; Rovira, I. I.; Cheng, H.-L.; Wang, G.; Gucek, M.; Lombard, D.; Alt, F. W.; Sack, M. N.; Murphy, E.; Cao, L.; Finkel, T., The NAD-dependent deacetylase SIRT2 is required for programmed necrosis. *Nature* **2012,** *492*, 199-204.

13. Purushotham, A.; Schug, T. T.; Xu, Q.; Surapureddi, S.; Guo, X.; Li, X., Hepatocyte-specific deletion of SIRT1 alters fatty acid metabolism and results in hepatic steatosis and inflammation. *Cell Metab.* **2009,** *9* (4), 327-338.

14. Chen, D.; Bruno, J.; Easlon, E.; Lin, S. J.; Cheng, H. L.; Alt, F. W.; Guarente, L., Tissue-specific regulation of SIRT1 by calorie restriction. *Genes Dev.* **2008,** *22* (13), 1753-1757.

15. Lara, E.; Mai, A.; Calvanese, V.; Altucci, L.; Lopez-Nieva, P.; Martinez-Chantar, M. L.; Varela-Rey, M.; Rotili, D.; Nebbioso, A.; Ropero, S.; Montoya, G.; Oyarzabal, J.; Velasco, S.; Serrano, M.; Witt, M.; Villar-Garea, A.; Imhof, A.; Mato, J. M.; Esteller, M.; Fraga, M. F., Salermide, a Sirtuin inhibitor with a strong cancer-specific proapoptotic effect. *Oncogene* **2009,** *28* (6), 781-791.

16. Trapp, J.; Meier, R.; Hongwiset, D.; Kassack, M. U.; Sippl, W.; Jung, M., Structure-activity studies on suramin analogues as inhibitors of NAD+-dependent histone deacetylases (sirtuins). *ChemMedChem* **2007,** *2* (10), 1419-1431.

17. Napper, A. D.; Hixon, J.; McDonagh, T.; Keavey, K.; Pons, J. F.; Barker, J.; Yau, W. T.; Amouzegh, P.; Flegg, A.; Hamelin, E.; Thomas, R. J.; Kates, M.; Jones, S.; Navia, M. A.; Saunders, J. O.; DiStefano, P. S.; Curtis, R., Discovery of indoles as potent and selective inhibitors of the deacetylase SIRT1. *J. Med. Chem.* **2005,** *48* (25), 8045-8054.

18. Sanders, B. D.; Jackson, B.; Brent, M.; Taylor, A. M.; Dang, W.; Berger, S. L.; Schreiber, S. L.; Howitz, K.; Marmorstein, R., Identification and characterization of novel sirtuin inhibitor scaffolds. *Bioorg. Med. Chem.* **2009,** *17* (19), 7031-7041.

19. Huhtiniemi, T.; Salo, H. S.; Suuronen, T.; Poso, A.; Salminen, A.; Leppänen, J.; Jarho, E.; Lahtela-Kakkonen, M., Structure-Based Design of Pseudopeptidic Inhibitors for SIRT1 and SIRT2. *J. Med. Chem.* **2011,** *54* (19), 6456-6468.

20. Kiviranta, P. H.; Suuronen, T.; Wallén, E. A. A.; Leppa□nen, J.; Tervonen, J.; Kyrylenko, S.; Salminen, A.; Poso, A.; Jarho, E. M., N-ε-Thioacetyl-Lysine-Containing Tri-, Tetra-, and Pentapeptides as SIRT1 and SIRT2 Inhibitors. *J. Med. Chem.* **2009,** *52* (7), 2153-2156.

21. Tervo, A. J.; Suuronen, T.; Kyrylenko, S.; Kuusisto, E.; Kiviranta, P. H.; Salminen, A.; Leppänen, J.; Poso, A., Discovering Inhibitors of Human Sirtuin Type 2: Novel Structural Scaffolds. *J. Med. Chem.* **2006,** *49*, 7239-7241.

22. Heltweg, B.; Gatbonton, T.; Schuler, A. D.; Posankony, J.; Li, H.; Goehlem, S.; Kollipara, R.; DePinho, R. A.; Gu, Y.; Simon, J. A.; Bedalov, A., Antitumor Activity of a Small-Molecule Inhibitor of Silent Information Regulator 2 Enzymes. *Cancer Res.* **2006,** *66* (8), 4368-4377.

23. Suzuki, T.; Khan, M. N. A.; Sawada, H.; Imai, E.; Itoh, Y.; Yamatsuta, K.; Tokuda, N.; Takeuchi, J.; Seko, T.; Nakagawa, H.; Miyata, N., Design, Synthesis, and Biological Activity of a Novel Series of Human Sirtuin-2-Selective Inhibitors. *J. Med. Chem.* **2012,** *55* (12), 5760-5773.

24. Fridén-Saxin, M.; Seifert, T.; Landergren, M. R.; Suuronen, T.; Lahtela-Kakkonen, M.; Jarho, E. M.; Luthman, K., Synthesis and Evaluation of Substituted Chroman-4-one and Chromone Derivatives as Sirtuin 2‑Selective Inhibitors. *J. Med. Chem.* **2012,** *55* (16), 7104-7113.

25. Galli, U.; Mesenzani, O.; Coppo, C.; Sorba, G.; Canonico, P. L.; Tron, G. C.; Genazzani, A. A., Identification of a Sirtuin 3 Inhibitor that Displays Selectivity of Sirtuins 1 and 2. *Eur. J. Med. Chem.* **2012,** *55*, 58-66.

26. Clark, M. A.; Acharya, R. A.; Arico-Muendel, C. C.; Belyanskaya, S. L.; Benjamin, D. R.; Carlson, N. R.; Centrella, P. A.; Chiu, C. H.; Creaser, S. P.; Cuozzo, J. W.; Davie, C. P.; Ding, Y.; Franklin, G. J.; Franzen, K. D.; Gefter, M. L.; Hale, S. P.; Hansen, N. J. V.; Israel, D. I.; Jiang, J.; Kavarana, M. J.; Kelley, M. S.; Kollmann, C. S.; Li, F.; Lind, K.; Mataruse, S.; Medeiros, P. F.; Messer, J. A.; Myers, P.; O'Keefe, H.; Oliff, M. C.; Rise, C. E.; Satz, A. L.; Skinner, S. R.; Svendsen, J. L.; Tang, L.; van Vloten, K.; Wagner, R. W.; Yao, G.; Zhao, B.; Morgan, B. A., Design, synthesis and selection of DNA-encoded small-molecule libraries. *Nat. Chem. Biol.* **2009,** *5* (9), 647-654.

27. Deng, H.; O'Keefe, H.; Davie, C. P.; Lind, K. E.; Acharya, R. A.; Franklin, G. J.; Larkin, J.; Matico, R.; Neeb, M.; Thompson, M. M.; Lohr, T.; Gross, J. W.; Centrella, P. A.; O'Donovan, G. K.; Bedard, K. L.; van Vloten, K.; Mataruse, S.; Skinner, S. R.; Belyanskaya, S. L.; Carpenter, T. Y.; Shearer, T. W.; Clark, M. A.; Cuozzo, J. W.; Arico-Muendel, C. C.; Morgan, B. A., Discovery of Highly Potent and Selective Small Molecule ADAMTS-5 Inhibitors That Inhibit Human Cartilage Degradation via Encoded Library Technology (ELT). *J. Med. Chem.* **2012,** *55* (16), 7061-7079.

28. Evindar, G.; Acharya, R. A.; Arico-Muendel, C. C.; Belyanskaya, S. L.; Brown, J.; Clark, M. A.; Centrella, P. A.; Cuozzo, J. W.; Davie, C. P.; Ding, Y.; Franklin, J. J.; Gross, J. W.; Israel, D. I.; Jolivette, L. J.; Jurewicz, A. J.; Lakdawala, A. S.; Li, F.; Li, H.; Lind, K. E.; Marino, J. P.; Morgan, B. A.; Messer, J. A.; Roethke, T. J.; Sargent, K. I.; Shewchuk, L. M.; Skinner, S. R.; Svendsen, J. L.; Xie, W.; Yang, H. In *Application of Encoded Library Technology (ELT) to the discovery of soluble epoxide hydrolase inhibitors*, 238th National Meeting of the American Chemical Society, Washington, DC, August 16-20, 2009; pp MEDI-126.

29. Graybill, T. L.; King, B. W.; Fosbenner, D. T.; Keller, P. M.; Morgan, B.; Clark, M. A.; Cuozzo, J. In *DNA-encoded libraries: A new resource for innovative hit identification*, 237th National Meeting of the American Chemical Society, Salt Lake City, UT, March 22-26, 2009; pp MEDI-297.

30. Davie, C. P.; Centrella, P. A.; O'Donovan, G. K.; Evindar, G.; O'Keefe, H.; Patel, A. M.; Clark, M. A. In *Design and synthesis of a sixteen million member DNA-encoded library (DEL) and discovery of potent Mycobacterium tuberculosis (Mtb) InhA inhibitors*, 240th National Meeting of the American Chemical Society, Boston, MA, United States, August 22-26, 2010; pp MEDI-150.

31. Ding, Y.; O'Keefe, H.; Svendsen, J. L.; Franklin, G. J.; Centrella, P. A.; Clark, M. A.; Acharya, R. A.; Li, F.; Messer, J. A.; Chiu, C. H.; Matico, R. E.; Murray-Thompson, M. F.; Skinner, S. R.; Belyanskaya, S. L.; Israel, D. I.; Cuozzo, J. W.; Arico-Muendel, C. C.; Morgan, B. A. In *Discovery of potent and selective inhibitors for ADAMTS-4 through encoded library technology (ELT)*, 240th National Meeting of the American Chemical Society, Boston, MA, August 22-26, 2010; pp MEDI-460.

32. Gentile, G.; Merlo, G.; Pozzan, A.; Bernasconi, G.; Bax, B.; Bamborough, P.; Bridges, A.; Carter, P.; Neu, M.; Yao, G.; Brough, C.; Cutler, G.; Coffin, A.; Belyanskaya, S., 5-Aryl-4-carboxamide-1,3-oxazoles: Potent and selective GSK-3 inhibitors. *Bioorg. Med. Chem. Lett.* **2012,** *22* (5), 1989-1994.

33. Jin, L.; Wei, W.; Jiang, Y.; Peng, H.; Cai, J.; Mao, C.; Dai, H.; Choy, W.; Bemis, J. E.; Jirousek, M. R.; Milne, J. C.; Westphal, C. H.; Perni, R. B., Crystal Structures of Human SIRT3 Displaying Substrate-induced Conformational Changes. *J. Biol. Chem.* **2009,** *284* (36), 24394-24405.

34. Dai, H.; Kustigian, L.; Carney, D.; Case, A.; Considine, T.; Hubbard, B. P.; Perni, R. B.; Riera, T. V.; Szczepankiewicz, B.; Vlasuk, G. P.; Stein, R. L., SIRT1 activation by small molecules - kinetic and biophysical evidence for direct interaction of enzyme and activator. *J. Biol. Chem.* **2010,** *285* (43), 32695–32703.

35. Stepanić, V.; Žiher, D.; Gabelica-Marković, V.; Jelić, D.; Nunhuck, S.; Valko, K.; Koštrun, S., Physicochemical profile of macrolides and their comparison with small molecules. *Eur. J. Med. Chem.* **2012,** *47*, 462-472.

36. Sanders, B. D.; Jackson, B.; Marmorstein, R., Structural basis for sirtuin function: What we know and what we don't. *Biochim. Biophys. Acta* **2010,** *1804* (8), 1604-1616.

37. Szczepankiewicz, B. G.; Dai, H.; Koppetsch, K. J.; Qian, D.; Jiang, F.; Mao, C.; Perni, R. B., Synthesis of Carba-NAD and the Structures of Its Ternary Complexes with SIRT3 and SIRT5. *J. Org. Chem.* **2012,** *77* (17), 7319-7329.

38. Avalos, J. L.; Bever, K. M.; Wolberger, C., Mechanism of Sirtuin Inhibition by Nicotinamide: Altering the NAD+ Cosubstrate Specificity of a Sir2 Enzyme. *Mol. Cell* **2005,** *17* (6), 855-868.

39. Finnin, M. S.; Donigian, J. R.; Pavletich, N. P., Structure of the histone deacetylase SIRT2. *Nat. Struct. Mol. Biol.* **2001,** *8* (7), 621-625.

40. Zhao, X.; Allison, D.; Condon, B.; Zhang, F.; Gheyi, T.; Zhang, A.; Ashok, S.; Russell, M.; macewan, I.; Qian, Y.; Jamison, J. A.; Luz, J. G., The 2.5 Å crystal structure of the SIRT1 catalytic domain bound to nicotinamide adenine dinucleotide (NAD+) and an indole (EX527 analog) reveals a novel mechanism of histone deacetylase inhibition. *J. Med. Chem.* **2013,** *56* (3), 963-969.

41. Winter, G., xia2: an expert system for macromolecular crystallography data reduction. *J. Appl. Crystallogr.* **2010,** *43* (1), 186-190.

42. Otwinowski, Z.; Minor, W., Processing of X-ray diffraction data collected in oscillation mode. In *Methods in Enzymology*, Carter, C. W.; Sweet, R. M., Eds. Academic Press: 1997; Vol. 276, pp 307-326.

43. McCoy, A. J.; Grosse-Kunstleve, R. W.; Adams, P. D.; Winn, M. D.; Storoni, L. C.; Read, R. J., Phaser crystallographic software. *J. Appl. Crystallogr.* **2007,** *40* (4), 658-674.

44. Murshudov, G. N.; Vagin, A. A.; Dodson, E. J., Refinement of macromolecular structures by the maximum-likelihood method. *Acta Cryst.* **1997,** *D53* (3), 240-255.

45. Winn, M. D.; Ballard, C. C.; Cowtan, K. D.; Dodson, E. J.; Emsley, P.; Evans, P. R.; Keegan, R. M.; Krissinel, E. B.; Leslie, A. G. W.; McCoy, A.; McNicholas, S. J.; Murshudov, G. N.; Pannu, N. S.; Potterton, E. A.; Powell, H. R.; Read, R. J.; Vagin, A.; Wilson, K. S., Overview of the CCP4 suite and current developments. *Acta Cryst.* **2011,** *D67* (4), 235-242.

46. Emsley, P.; Cowtan, K., Coot: model-building tools for molecular graphics. *Acta Cryst.* **2004,** *D60* (Pt 12 Pt 1), 2126-2132.

47. Leslie, A. G. W., *Joint CCP4 and ESF-EACBM Newsletter on Protein Crystallography* **1992,** (27), 30.

48. Evans, P., Scaling and assessment of data quality. *Acta Cryst.* **2006,** *D62* (1), 72-82.

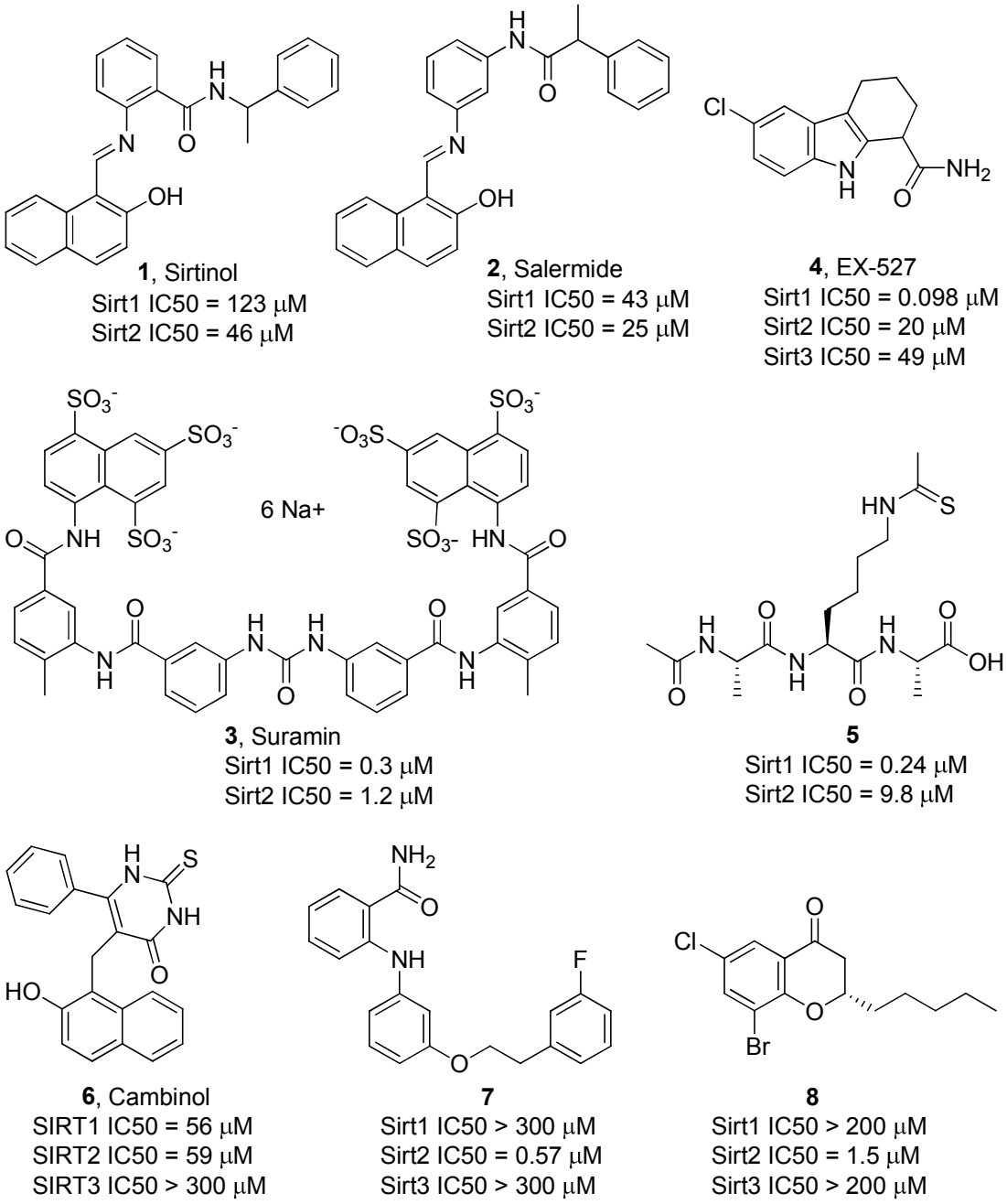

Figure 1. Sirtuin inhibitors reported in the literature.

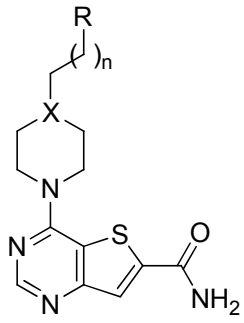

9

Figure 2. General structure of thieno[3,2-*d*]pyrimidine-6-carboxamide SIRT1/2/3 pan-inhibitors.

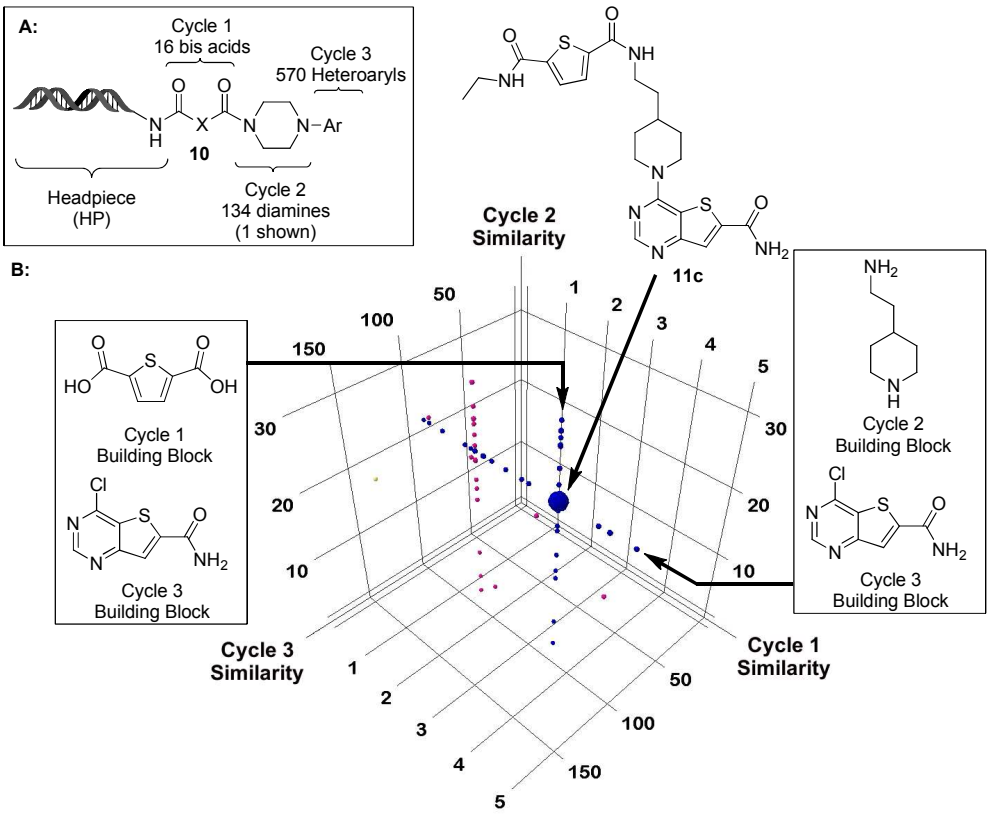

Figure 3. SIRT3 ELT affinity screen of a 1.2 million library. (a) General structure for the 3-cycle linear ELT screening library. (b) Spotfire™ cube data visual analysis from the SIRT3 ELT affinity screen. Selected SIRT3 features are represented by points in a 3D cube, with each point representing a unique selected molecule. Common building blocks (in boxes) are defined by lines. A plane is observed for the common cycle 3 building block (4-chlorothieno[3,2-d]pyrimidine-6-carboxamide). The intersection of the cycle 1 and cycle 2 lines translates into the representative compound **11c**.

Scheme 1. Synthetic methods to prepare **11a - d**[a]

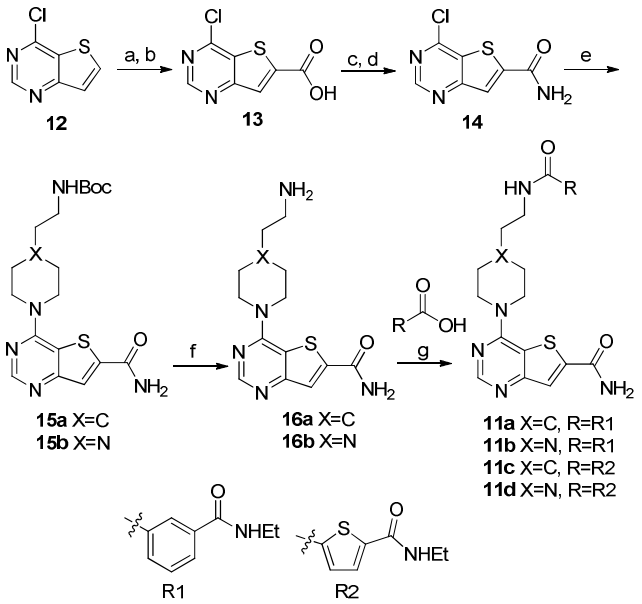

[a] Conditions: (a) 2,2,6,6-Tetramethylpiperidine, n-BuLi, THF, -78 ºC; (b) CO_2, -78 ºC to RT; (c) oxalyl chloride, DMF, CH_2Cl_2 reflux; (d) 0.5 M NH_3 in dioxane; (e) 4-(2-Boc-aminoethyl)piperidine (for **15a**) or 4-(2-Boc-aminoethyl)piperazine (for **15b**), DIEA, CH_3CN, 85 ºC; (f) TFA/CH_2Cl_2; (g) HATU, DIEA, 3-(ethylcarbamoyl)benzoic acid (for **11a** and **11b**) or 5-(ethylcarbamoyl)thiophene-2-carboxylic acid (for **11c** and **11d**).

Table 1. Sirtuin inhibition activity of off-DNA ELT screening hits.

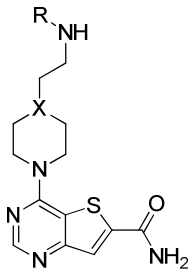

Cmpd	R	X	IC_{50} (μM)[i]			LogD[ii]	Solubility[iii] (μM)	MW	CLogP	tPSA
			SIRT1	SIRT2	SIRT3					
11a	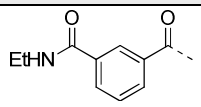	CH	0.0053	0.0013	0.0049	2.09	19	481	2.16	129
11b		N	0.067	0.010	0.024	1.45	220	482	1.74	132
11c	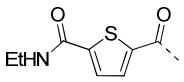	CH	0.0036	0.0027	0.0040	2.09	9	487	1.92	129
11d		N	0.031	0.0048	0.023	1.32	65	488	1.50	132

[1] IC_{50} values were determined from three separate titration curves. Each of the IC50 values shown represents the mean of at least three determinations, with variation in individual values of < 50%. [ii] LogD was determined by a HPLC based lipophilicity assay[35] by measuring Chromatographic Hydrophobicity Index (CHI) values by reverse phase HPLC and transforming them to a LogD scale based on known standards. [iii] Kinetic solubility was determined by a Chemi-Luminescent Nitrogen Detection (CLND) solubility assay.[35] DMSO stock solutions were incubated (1 hr) in phosphate buffered saline (pH 7.4), filtered and measured by CLND.

Table 2. SIRT 1/2/3 inhibition of truncated analogs of **11c.**

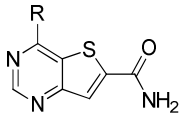

Cmpd	R	IC_{50} (μM)[1]		
		SIRT1	SIRT2	SIRT3
11c	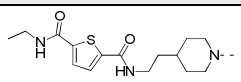	0.0036	0.0027	0.0040
17	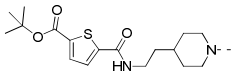	0.0067	0.0018	0.0032
18	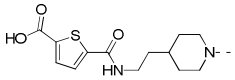	0.014	0.0044	0.013
19	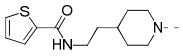	0.0058	0.0065	0.0076
15a	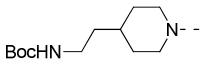	0.017	0.0054	0.029
20	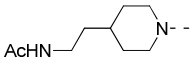	0.11	0.023	0.056
16a	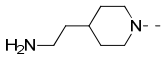	1.6	0.11	0.30
21		15	1.4	8.6
22	EtNH-	>50	49	>50
14	Cl-	>50	>50	>50

[1] IC_{50} values were determined from three separate titration curves. Each of the IC_{50} values shown represents the mean of at least three determinations, with variation in individual values of < 50%.

Table 3. Effect of aliphatic functionality and linker length on SIRT 1/2/3 inhibition.

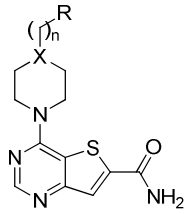

Cmpd	R	X	n	IC_{50} (μM)[i]		
				SIRT1	SIRT2	SIRT3
4	-	-	-	0.26	2.9	>50
23	-NH(C=O)Me	CH	1	16	2.8	4.4
20	-NH(C=O)Me	CH	2	0.11	0.023	0.056
24	-NH(C=O)Me	N	2	1.6	0.17	0.77
25	-NH(C=S)Me	CH	2	0.056	0.030	0.039
26	-NH(C=S)Me	N	2	0.49	0.13	0.28
27	-NH(C=O)*t*Bu	CH	1	4.3	0.74	0.65
28	-NH(C=O)*t*Bu	CH	2	0.015	0.010	0.033
29	-NH(C=O)*t*Bu	CH	3	0.042	0.016	0.067
30	-NH(C=O)*t*Bu	N	2	0.12	0.017	0.092
31	$-NHSO_2Me$	CH	2	0.0043	0.0011	0.0072
32	$-NHSO_2Me$	N	2	0.38	0.053	0.37
33		CH	1	0.73	0.22	0.061
34		CH	2	0.11	0.067	0.028
35		N	2	0.053	0.029	0.030

[1] IC_{50} values were determined from three separate titration curves. Each of the IC_{50} values shown represents the mean of at least three determinations, with variation in individual values of < 50%.

Table 4. Effect of modification of the thieno[3,2-*d*]pyrimidine core on SIRT1/2/3 inhibition.

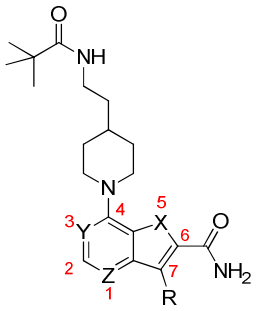

Cmpd	X	Y	Z	R	IC_{50} (μM)[i]		
					SIRT1	SIRT2	SIRT3
28	S	N	N	H	0.015	0.010	0.033
36	O	N	N	H	0.47	0.15	1.3
37	S	CH	N	H	0.059	0.028	0.11
38	S	N	CH	H	0.49	0.30	2.1
39	S	N	N	Me	0.18	0.13	0.15

[i] IC_{50} values, expressed in μM, were determined from three separate titration curves. Each of the IC_{50} values shown represents the mean of at least three determinations, with variation in individual values of < 50%. Ring atom numbering is depicted in red.

Table 5. Effect of modification of the 6-carboxamide on SIRT1/2/3 inhibition.

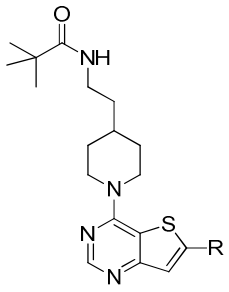

Cmpd	R	IC50 (μM)[i]		
		SIRT1	SIRT2	SIRT3
28	-(C=O)NH_2	0.015	0.010	0.033
40	-(C=O)OH	>50	>50	>50
41	-(C=O)NHMe	>50	10	>50
42	-H	>50	>50	>50

[i] IC_{50} values were determined from three separate titration curves. Each of the IC_{50} values shown represents the mean of at least three determinations, with variation in individual values of < 50%.

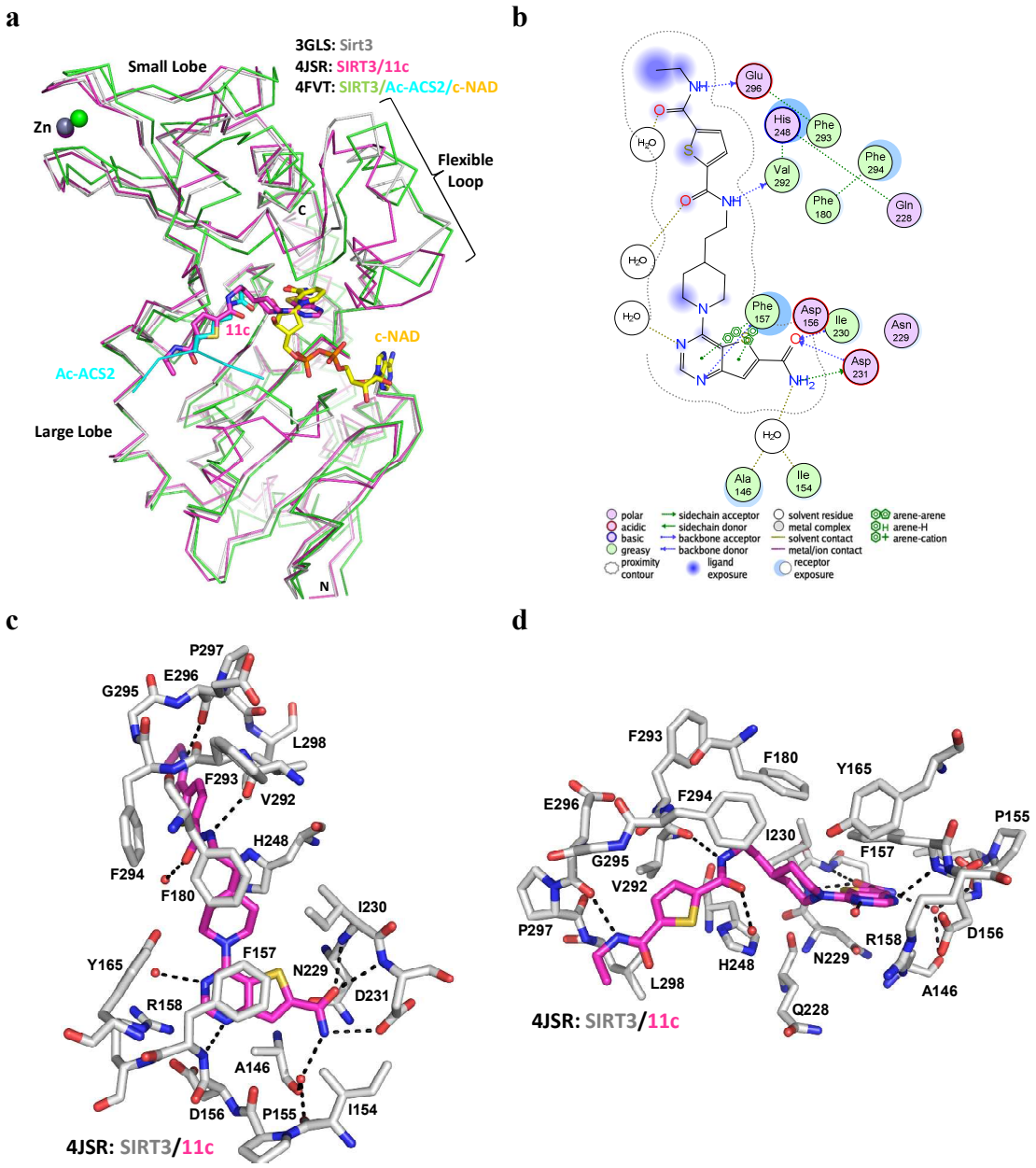

Figure 4. Crystal structure of SIRT3(118-399) bound with **11c**. (a) Structural comparison of apo SIRT3 (grey), SIRT3/**11c** (magenta), and the ternary complex of SIRT3 (green)/carba-NAD^+ (yellow)/Ac-ACS2 peptide (cyan). SIRT3 protein is represented as alpha carbon lines, whereas the N-epsilon acetyl lysine of Ac-ACS2, **11c** and carba-NAD are represented as sticks. (b) Ligand interaction map of SIRT3/**11c**. (c) Active site view of the crystal structure of SIRT3 (grey)/**11c** (magenta). (d) Substrate channel view of SIRT3/**11c** crystal structure.

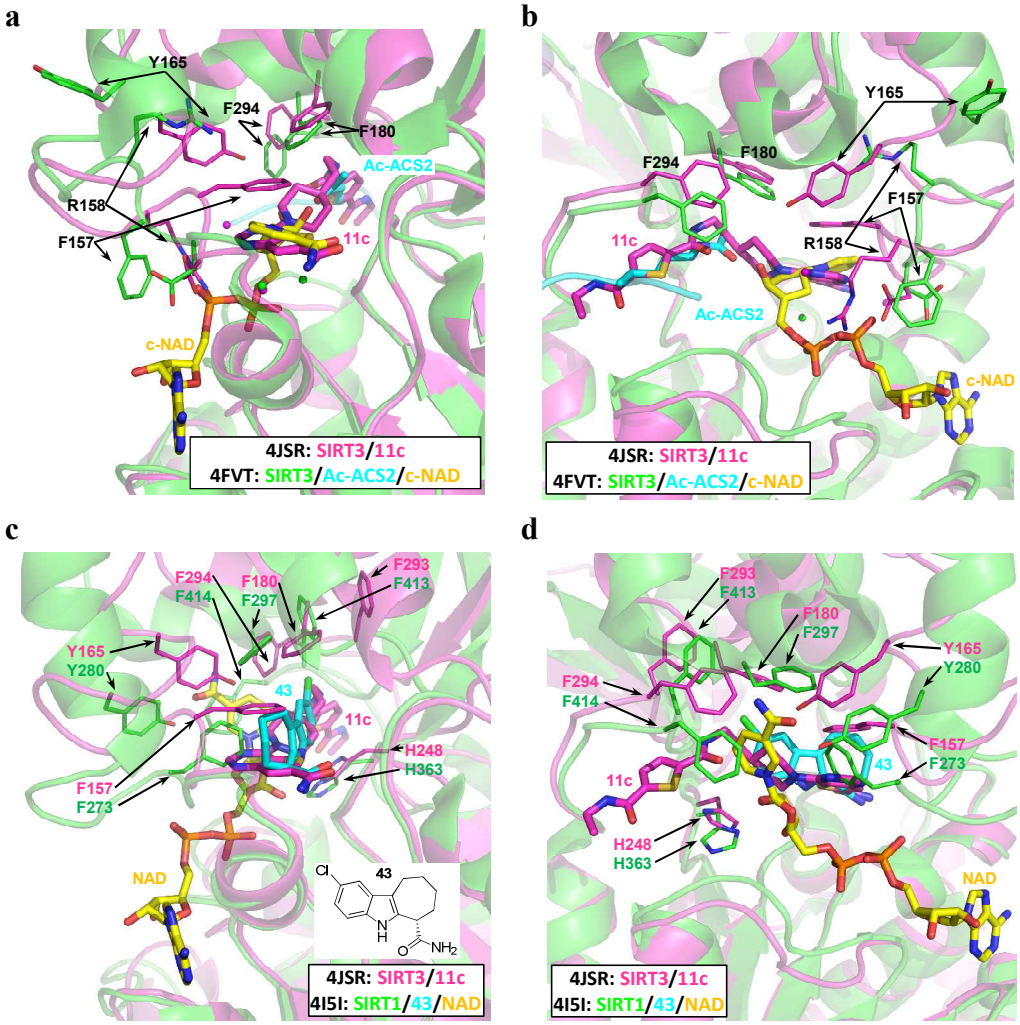

Figure 5. Structural comparison of SIRT3/**11c** vs. SIRT3/carba-NAD/ACS2 and catalytic core of SIRT1/NAD/**43**. (a) Active site view of the structural comparison of SIRT3/**11c** (magenta) and the ternary complex of SIRT3 (green), carba-NAD^+ (yellow) and Ac-ACS2 peptide (cyan). (b) Substrate channel view of the comparison of SIRT3/**11c** and the ternary complex of SIRT3/carba-NAD^+/Ac-ACS2. (c) Active site view of the structural comparison of SIRT3/**11c** (magenta) and the ternary complex of SIRT1 (green), NAD^+ (yellow) and **43** (cyan). (d) Substrate channel view of the comparison of SIRT3/**11c** and the ternary complex of SIRT1/NAD^+/**43**.

TABLE OF CONTENTS FIGURE

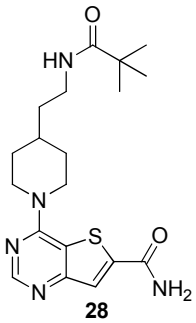

28

SIRT1 IC_{50} = 15 nM
SIRT2 IC_{50} = 10 nM
SIRT3 IC_{50} = 33 nM

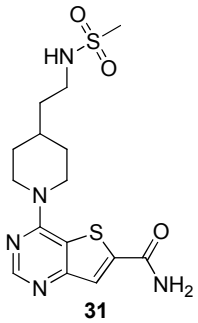

31

SIRT1 IC_{50} = 4 nM
SIRT2 IC_{50} = 1 nM
SIRT3 IC_{50} = 7 nM